

AD-A054 961

AIR FORCE GEOPHYSICS LAB HANSCOM AFB MASS
EQUATORIAL IRREGULARITY CAMPAIGNS. PART I. CORRELATED SCINTILLA--ETC(U)
NOV 77 S BASU, J AARONS
AFGL-TR-77-0264

F/G 20/14

UNCLASSIFIED

NL

1 OF 1
AD
A054961



END
DATE
FILMED
7-78
DDC

AD A 054961

FOR FURTHER TRAN

AFGL-TR-77-0264
ENVIRONMENTAL RESEARCH PAPERS, NO. 617

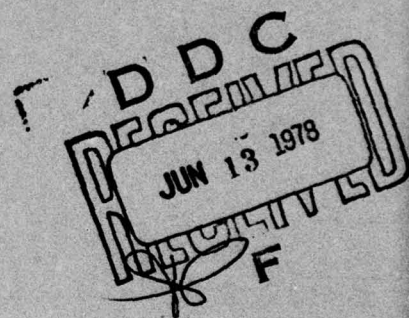
12
B.S.



**Equatorial Irregularity Campaigns
Part I: Correlated Scintillation and Radar
Backscatter Measurements in October 1976**

SANTIMAY BASU
JULES AARONS

23 November 1977



Approved for public release; distribution unlimited.

AD No. _____
DDC FILE COPY

SPACE PHYSICS DIVISION PROJECT 4643
AIR FORCE GEOPHYSICS LABORATORY
HANSCOM AFB, MASSACHUSETTS 01731

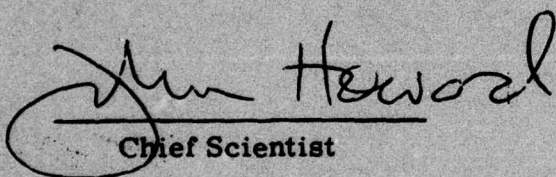
AIR FORCE SYSTEMS COMMAND, USAF



This report has been reviewed by the ESD Information Office (OI) and is releasable to the National Technical Information Service (NTIS).

This technical report has been reviewed and is approved for publication.

FOR THE COMMANDER


Chief Scientist

Qualified requestors may obtain additional copies from the Defense Documentation Center. All others should apply to the National Technical Information Service.

Unclassified

SECURITY CLASSIFICATION OF THIS PAGE (When Data Entered)

REPORT DOCUMENTATION PAGE		READ INSTRUCTIONS BEFORE COMPLETING FORM	
1. REPORT NUMBER	2. GOVT ACCESSION NO.	3. RECIPIENT'S CATALOG NUMBER	
14 AFGL-TR-77-0264	AFGL-ERP-617		
4. TITLE (and Subtitle)	5. TYPE OF REPORT & PERIOD COVERED		
6 EQUATORIAL IRREGULARITY CAMPAIGNS. PART I. CORRELATED SCINTILLATION AND RADAR BACKSCATTER MEASUREMENTS IN OCTOBER 1976 .	Scientific Interim rept.		
7. AUTHOR(s)	6. PERFORMING ORG. REPORT NUMBER		
10 Santimay Basu Jules/Aarons	ERP, No. 617		
	8. CONTRACT OR GRANT NUMBER(s)		
9. PERFORMING ORGANIZATION NAME AND ADDRESS	10. PROGRAM ELEMENT, PROJECT, TASK AREA & WORK UNIT NUMBER		
Air Force Geophysics Laboratory (PHP) Hanscom AFB, Massachusetts 01731	62101F 46430502 17/05		
11. CONTROLLING OFFICE NAME AND ADDRESS	12. REPORT DATE		
Air Force Geophysics Laboratory (PHP) Hanscom AFB, Massachusetts 01731	23 November 1977		
	13. NUMBER OF PAGES		
	50		
14. MONITORING AGENCY NAME & ADDRESS (if different from Controlling Office)	15. SECURITY CLASS. (of this report)		
	Unclassified 12/57p		
	15a. DECLASSIFICATION/DOWNGRADING SCHEDULE		
16. DISTRIBUTION STATEMENT (of this Report)			
Approved for public release; distribution unlimited.			
17. DISTRIBUTION STATEMENT (of the abstract entered in Block 20, if different from Report)			
18. SUPPLEMENTARY NOTES			
This work was performed in cooperation with Emmanuel College under Contract AF 19628-76-C-0003 and was partially supported by SAMSO under Procurement Directive 77-12. *Emmanuel College, Boston, Mass. 02115			
19. KEY WORDS (Continue on reverse side if necessary and identify by block number)			
Ionospheric scintillations Irregularity drift velocities Equatorial region Irregularity sizes F-region irregularities Jicamarca backscatter radar			
20. ABSTRACT (Continue on reverse side if necessary and identify by block number)			
An intensive study of nighttime electron density irregularities in the equatorial ionosphere was conducted in October 1976 by making simultaneous radar and scintillation measurements near the magnetic dip equator. The 50-MHz radar observations at Jicamarca, Peru, and scintillation measurements at nearby ground stations of Ancon and Huancayo, Peru, were made by receiving VHF transmissions from the geostationary satellites, LES-9 and Marisat, as well as the VHF transmissions from the orbiting Wideband satellite. The thick irregularity patches detected by the radar could be associated with intense			

DDC
RECEIVED
JUN 13 1978
RESERVED
F

DD FORM 1 JAN 73 1473 EDITION OF 1 NOV 65 IS OBSOLETE

Unclassified

SECURITY CLASSIFICATION OF THIS PAGE (When Data Entered)

409 578 Gu

Unclassified

SECURITY CLASSIFICATION OF THIS PAGE(When Data Entered)

20. (Cont)

scintillation events, signifying thereby that the patches containing 3-m irregularities also contain kilometer-sized irregularities, giving rise to the radar backscatter and scintillations, respectively. By comparison of the onset times of scintillation on different propagation paths separated in the east-west direction, as well as by performance of spaced receiver scintillation measurements at Ancon, the drift speed of irregularities was determined. The irregularities were observed to drift eastwards at a speed ranging between 90 and 140 m per sec during 1900 and 2400 local time. From a knowledge of the derived value of drift speed and the duration of scintillation events, the irregularity patches were found to have eastward dimensions between 100 and 800 kilometers.

On a statistical basis, the irregularity patches detected in the scintillation experiment were noted to be preponderant to those giving rise to thick radar backscatter structures. This indicates the possibility of having equatorial irregularity patches with spectral powers concentrated at large scale sizes only.

Unclassified

SECURITY CLASSIFICATION OF THIS PAGE(When Data Entered)

Preface

A report such as this could not be accomplished without the dedicated efforts of many experimenters and collaboration of various institutions. The authors thank the Instituto Geofísico del Perú for their help in recording the data as well as for their hospitality towards the visiting scientists. The assistance of Herbert E. Whitney, John P. Mullen, Jurgen Buchau (Air Force Geophysics Laboratory) and Allen Johnson (Air Force Avionics Laboratory) in making scintillation observations and reducing their data is gratefully acknowledged. The authors thank J. Phil McClure of the University of Texas at Dallas, for performing the radar backscatter observations in collaboration with the staff of the Jicamarca Radar Observatory, and for placing the data at our disposal. Thanks are due to Sunanda Basu for her comments on the manuscript, together with stimulating discussions in the course of preparation of this report. The authors also acknowledge the assistance of M. Patricia Hagan and the Emmanuel College Physics Research Division.

ACCESSION for	
NTIS	Whole Section <input checked="" type="checkbox"/>
DGC	Part Section <input type="checkbox"/>
UNANNOUNCED <input type="checkbox"/>	
JUST NOTICE	
BY	
DISTRIBUTION/AVAILABILITY CODES	
1	SPECIAL
A	

Contents

1. INTRODUCTION	9
2. OBSERVATIONS	11
2.1 Ground Measurements	11
2.2 Airborne Measurements	13
3. RELATIONSHIPS BETWEEN IRREGULARITY PARAMETERS, SCINTILLATION INDEX, AND BACKSCATTERED POWER	14
3.1 Irregularity Parameters and Scintillations	14
3.2 Irregularity Parameters and Radar Backscatter	17
4. RESULTS	18
4.1 Observations Made on 16-17 October 1976	18
4.2 Observations Made on 18-19 October 1976	22
4.3 Observations Made on 19-20 October 1976	26
4.4 Observations Made on 20-21 October 1976	31
4.5 Observations Made on 21-22 October 1976	32
4.6 Observations Made on 24-25 October 1976	35
4.7 Observations Made on 29-30 October 1976	38
4.8 Wideband Satellite Observations	44
5. DISCUSSION	45
REFERENCES	49

Illustrations

1.	Geometry of Simultaneous Radar and Scintillation Measurements	12
2(a).	The 50-MHz Radar Backscattered Power Map of Nighttime Irregularities Obtained at Jicamarca on 16-17 October 1976	19
2(b).	Temporal Variation of 249-MHz Scintillation Index SI(dB), and Fading Rate Recorded on 16-17 October 1976, at Ancon on the Propagation Path to LES-9	20
2(c).	Temporal Variation of 249-MHz Scintillation Index SI(dB), and Fading Rate Recorded on 16-17 October 1976, at Huancayo on the Propagation Path to LES-9	22
3(a)-1.	Radar Backscattered Power Map Recorded at Jicamarca Between 1930-2210 LT on 18-19 October 1976	23
3(a)-2.	Radar Backscattered Power Map Between 2120-0040 LT on 18-19 October 1976	24
3(b).	Temporal Variation of 249-MHz Scintillation Index, SI(dB) and Fading Rate Recorded at Ancon by the Use of LES-9 Satellite on 18-19 October 1976	24
3(c).	Temporal Variation of 249-MHz Scintillation Index, SI(dB) and Fading Rate Recorded at Huancayo by the Use of LES-9 Satellite on 18-19 October 1976	25
3(d).	Temporal Variation of 257-MHz Scintillation Index, SI(dB) Recorded at Huancayo with Marisat Satellite on 18-19 October 1976	25
4(a).	Radar Backscattered Power Map Obtained at Jicamarca on 19-20 October 1976	27
4(b).	Temporal Variation of Scintillation Index and Fading Rate of 249-MHz Transmissions from LES-9 Recorded at Ancon on 19-20 October 1976	27
4(c).	Temporal Variation of Scintillation Index and Fading Rate of 249-MHz Transmissions from LES-9 Recorded at Huancayo on 19-20 October 1976	28
4(d).	Variation of Scintillation Index of 257-MHz Transmissions from Marisat Recorded at Huancayo on 19-20 October 1976	28
4(e).	Subionospheric Flight Path of the AFGL Aircraft Making 249-MHz Scintillation Observations with LES-9 on 19-20 October 1976	29
5(a)-1.	Backscattered Power Map Obtained at Jicamarca Between 1910-2220 LT on 20-21 October 1976	31
5(a)-2.	Backscattered Power Map Between 2050-2320 LT on 20-21 October 1976	32
6(a)-1.	Backscattered Power Map Obtained at Jicamarca Between 1940-2240 LT on 21-22 October 1976	33
6(a)-2.	Backscattered Power Map Between 2050-2350 LT on 21-22 October 1976	33

Illustrations

6(b).	Scintillation Index and Fading Rate of 249-MHz Transmissions from LES-9 Recorded at Ancon on 21-22 October 1976	34
6(c).	Scintillation Index and Fading Rate of 249-MHz LES-9 Transmissions Recorded at Huancayo on 21-22 October 1976	34
6(d).	Scintillation Index of Marisat Transmissions at 257 MHz Recorded at Huancayo on 21-22 October 1976	35
7(a)-1.	Backscattered Power Map Obtained at Jicamarca Between 2040-0010 LT on 24-25 October 1976	36
7(a)-2.	Backscattered Power Map Between 2220-0220 LT on 24-25 October 1976	36
7(a)-3.	Backscattered Power Map Between 0030-0400 LT on 24-25 October 1976	37
7(b).	Scintillation Index and Fading Rate of 249-MHz Transmissions from LES-9 Recorded at Ancon on 24-25 October 1976	37
7(c).	Scintillation Index and Fading Rate of 249-MHz Transmissions from LES-9 Recorded at Huancayo on 24-25 October 1976	38
8(a)-1.	Backscattered Power Map Obtained at Jicamarca Between 1930-2240 LT on 29-30 October 1976	39
8(a)-2.	Backscattered Power Map Between 2130-0120 LT on 29-30 October 1976	39
8(a)-3.	Backscattered Power Map Between 0040-0400 LT on 29-30 October 1976	40
8(b).	Scintillation Index and Fading Rate of 249-MHz Transmissions from LES-9 Recorded at Ancon on 29-30 October 1976	40
8(c).	Scintillation Index and Fading Rate of 249-MHz Transmissions from LES-9 Recorded at Huancayo on 29-30 October 1976	41
8(d).	Comparison of Backscattered Power Map and ATS-6 Scintillation Data Corresponding to a Common Ionospheric Volume Obtained on 29-30 October 1976	42
9.	Comparison of Backscattered Power Maps in Schematic Form, and Scintillation Results During the Period of Simultaneous Measurements in October 1976	43
10.	Subionospheric Tracks of Wideband Satellite Transits Recorded at Huancayo During October 1976	45

Tables

1.	List of Stations and Experiments Performed During 16-30 October 1976	14
2.	Drift Velocities and East-West Dimensions of Irregularity Patches	44

Equatorial Irregularity Campaigns Part I: Correlated Scintillation and Radar Backscatter Measurements in October 1976

1. INTRODUCTION

For several decades, the nighttime F-region irregularities of electron density at equatorial latitudes have been studied by observing the spread-F signature on ionograms and scintillations in transionospheric communication links.¹⁻³ The results of these studies established the existence of a narrow belt of strong F-region irregularities in the equatorial region, but they failed to provide an insight into the physical mechanisms of irregularity generation. Craft and Westerlund⁴ reported that a substantial amount of scintillation occurs at frequencies as high as several gigahertz in practical communication systems operating over the equatorial region. This was unexpected in the context of prevailing theories and thus provided an incentive to further studies of the problem. In recent years, a variety of new and

(Received for publication 22 November 1977)

1. Booker, H. G., and Wells, H. W. (1938) Scattering of radio waves by the F-region of the ionosphere, *J. Geophys. Res.* **43**:249-256.
2. Aarons, J. Whitney, H. E., and Allen, R. S. (1971) Global morphology of ionospheric scintillation, *Proc. IEEE* **59**:159-172.
3. Skinner, N. J., and Kelleher, R. F. (1971) Studies of F-region irregularities at Nairobi, I - From spread-f on ionograms 1964-1970, *Ann. Geophys.* **27**:181-194.
4. Craft, H. D., and Westerlund, L. H. (1972) Scintillation at 4 and 6 GHz caused by the ionosphere, AIAA Paper No. 72-179, American Institute of Aeronautics and Astronautics Library, New York.

powerful experimental techniques, such as measurements by rockets and satellites, HF forward scatter and VHF radar backscatter measurements have been employed to explore the equatorial irregularities.

The satellite in situ measurements have shown that the equatorial F-region irregularities occur in regions of large scale plasma depletions with an abundance of molecular ions and that the irregularities exhibit an upward and westward component of plasma motion.^{5,6*} These measurements also indicate that the nighttime irregularities of electron density at F-region heights can be of the same order as the mean density⁷ and that the one-dimensional irregularity wavenumber (k) spectrum follows a k^{-1} law from a few kilometers to a few tens of meters.⁸ By utilizing the above wave number spectrum and the in situ measurements of electron density deviation, Basu et al⁹ have developed the morphology of equatorial scintillations and demonstrated a pronounced longitude variation of these scintillations.

The rocket measurements of the equatorial irregularities at F-region heights corroborated the power law variation of irregularity power spectrum^{10,11} as established by satellites; Kelley et al¹⁰ obtained evidence of irregularity transport from the bottomside to the topside ionosphere during the development phase. This lends support to the currently proposed theoretical mechanisms of initial development of holes in the marginally stable bottomside ionosphere and their upward transport by means of buoyancy forces well into the stable topside ionosphere.

The 50-MHz radar backscatter experiment performed at Jicamarca, Peru, has recently employed the digital power mapping technique of the backscatter echoes from 3-m irregularities. These maps reveal the existence of 3-m irregularity structures rising from the bottomside ionosphere well into the topside.¹² The irregularity structures are usually observed to be tilted towards the west and found at times to occur at periodic intervals. The HF forward scatter experiments performed earlier in the equatorial region gave evidence of irregularity patches existing in quasi-periodic patterns and extending hundreds of kilometers in the east-west direction.¹³

These experimental investigations have been supported by computer simulations¹⁴ and analytic work on the formation of equatorial irregularities.^{15,16} Haerendel¹⁵ has shown that a four-step hierarchy of instabilities starting with collision-dominated Rayleigh-Taylor and ending with driftwave instability can explain the generation of nighttime equatorial irregularities having scale sizes from tens of kilometers to a few meters. On the other hand, Hudson and Kennel¹⁶ show that meter-wave irregularities can be directly generated by driftwave instability mechanisms.

* Because of the number of references appearing on this page, footnotes will not be included. See References, p. 49.

Basu and Kelley¹⁷ have recently reviewed the foregoing theoretical and experimental studies and concluded that they have considerably improved our understanding of the nighttime equatorial irregularities. However, these authors point out that some of the basic questions remain unresolved. For example, it has not been established if the generation mechanism is related to the passage of the terminator (or sunset line), or to the existence of suitable local conditions in certain spatial locations. The nighttime equatorial irregularities exhibit marked day-to-day variability. A night showing the presence of intense irregularities may be followed by another characterized by a total absence of irregularities. Finally, the relationship between the meter-sized irregularities causing the VHF radar backscatter, and the kilometer-sized irregularities, giving rise to VHF and UHF scintillations has not been sufficiently explored.

In view of the foregoing objectives, an intensive study of equatorial irregularities was undertaken during 16-30 October 1976. During this period, the 50-MHz radar backscatter experiments were conducted at Jicamarca, and simultaneous scintillation measurements were made at two nearby ground stations (Ancon and Huancayo, both in Peru) with geostationary and orbiting satellites. In addition, aircraft were employed to make on-board scintillation experiments providing spatial configuration of irregularity patches. Multistation scintillation measurements were used to study the localized origin of large scale irregularity patches, their drift speed, spatial extent, and lifetime in the equatorial ionosphere. The simultaneous radar and scintillation observations also provided information on the relationship between the meter- and kilometer-sized irregularities, giving rise to the radar backscatter and VHF-UHF scintillations, respectively.

2. OBSERVATIONS

2.1 Ground Measurements

The 50-MHz radar was operated at Jicamarca (11.97°S, 76.86°W) by J. P. McClure in collaboration with the staff of the Instituto Geofísico del Perú, and the radar maps were made available to us. These maps providing range and intensity of the backscattered power as a function of time were acquired by employing digital power mapping techniques. A complete description of the radar and the mapping technique has been outlined by Woodman and La Hoz.¹² In view of the high aspect sensitivity of equatorial irregularities and 2°N magnetic dip location of Jicamarca, the radar beam is oriented slightly off-vertical in order to obtain the backscattered

17. Basu, Sunanda, and Kelley, M.C. (1977) Review of equatorial scintillation phenomena in the light of recent developments in the theory and measurement of equatorial irregularities, *J. Atmos. Terr. Phys.* 39:1229-1242.

echoes. The geometry of the radar and scintillation measurements is illustrated in Figure 1. The locations of the ground stations, Jicamarca (JI), Ancon (AN), and Huancayo (HU) are indicated in the diagram.

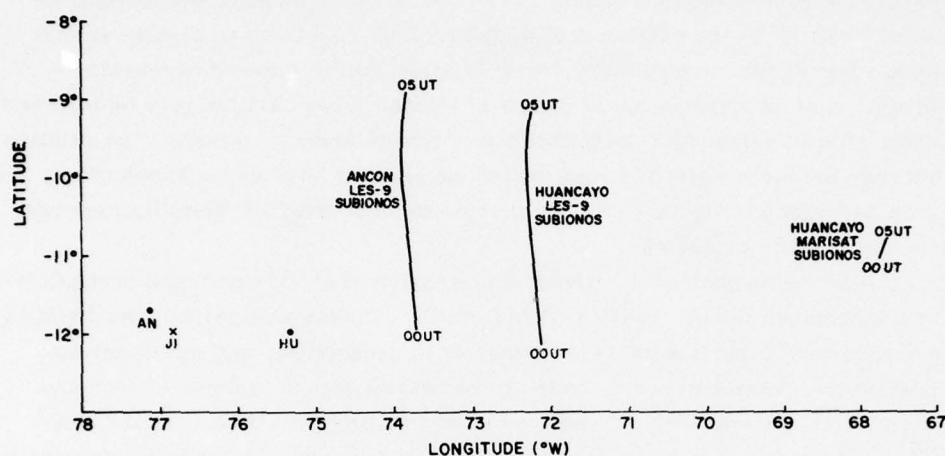


Figure 1. Geometry of Simultaneous Radar and Scintillation Measurements. JI, AN, and HU signify ground locations of Jicamarca, Ancon, and Huancayo

Scintillation measurements were made at Ancon (11.7°S , 77.15°W) by the use of 249-MHz transmissions from the geostationary satellite, LES-9. In view of the finite orbital inclination of LES-9, the intersection of the propagation path from Ancon to LES-9 with a given ionospheric height did not remain fixed but traced out a curve with varying time, the locus remaining nearly parallel to a longitude circle. Figure 1 shows the position of Ancon (AN) ground station, as well as the locus of the subionospheric point of LES-9 observations on 17 October 1976, referred to a height of 400 km. The elevation angle of the satellite, as viewed from Ancon, varied from 44° to 36° between 00 UT and 05 UT.

Spaced receiver scintillation measurements were conducted at Ancon by employing two independent receiving systems with their antennas located on an east-west baseline of 366 m. Each receiving system was comprised of a high gain antenna, low noise converter and R-390 receiver with an over-all bandwidth of 2 kHz and a post-detection integrating circuit of time constant 0.1 sec. The detected signal after integration was recorded on strip chart recorders, as well as on FM analog tapes. The strip chart records were analyzed manually to obtain the scintillation index, SI(dB) at every 2-min interval.¹⁸ The FM analog tapes were later

18. Whitney, H.E., Aarons, J., and Malik, C. (1969) A proposed index for measuring ionospheric scintillations, *Planet. Space. Sci.* 17:1069-1073.

digitized for special investigations, such as the determination of theory-based S_4 index of scintillation,¹⁹ the power spectrum of scintillations or the drift speed of irregularities from a cross-correlation analysis of spaced receiver scintillation data.

At Huancayo (11.97°S, 75.34°W), the scintillation measurements were made by the use of 249-MHz transmissions from LES-9 as well as Marisat transmissions at 257 and 1541 MHz. The elevation angle of LES-9, as viewed from Huancayo, varied from 46° to 38° between 00 UT to 05 UT, whereas the elevation angle of Marisat observations varied between 20.8° and 21.2° during the same time interval. We shall discuss only the 257-MHz scintillation observations from Marisat, as this frequency closely corresponds to LES-9 transmissions. From Figure 1, the location of the Huancayo (HU) ground station may be noted as well as the loci of the subionospheric points of LES-9 and Marisat observations between 00 UT and 05 UT on 17 October 1976. The scintillation measurements at Huancayo were performed with the two satellites, in order to explore simultaneously the two ionospheric volumes well separated in longitude. During the period of observations, the ATS-6 satellite could also be viewed from Huancayo, while it was drifting westwards to its new location. On 29 October 1976, the propagation path from Huancayo to the ATS-6 satellite intersected the ionosphere over Jicamarca and scintillation measurements with ATS-6 transmissions at 137 and 360 MHz were made at Huancayo. This offered an opportunity to explore quantitatively the relationship between the radar and scintillation measurements, as will be discussed in Section 3.2. As at Ancon, all scintillation data were acquired on both strip chart recorders and FM analog tapes. In addition to the above scintillation measurements with geostationary satellites, the orbiting Wideband satellite was also used to perform 137-MHz scintillation measurements from Huancayo. The orbiting satellite observations yielded the spatial configuration of the irregularities.

2.2 Airborne Measurements

Two aircraft were flown by the Air Force Geophysics Laboratory (AFGL) and the Air Force Avionics Laboratory (AFAL) in order to perform scintillation measurements with the 249-MHz beacon from LES-9. The aircraft flew between the ground stations and explored the spatial configuration of irregularity structures causing scintillations. The AFGL aircraft also carried an ionosonde providing digital ionograms, and made airglow observations at 6300 Å. In this report, we shall, however, deal with the results of aircraft scintillation measurements on a few specific nights. The LES-9 scintillation measurements made on board the aircraft explored the ionospheric locations between approximately 10°S and 13°S over a longitude interval of 72°W and 76°W.

19. Briggs, B. H., and Parkin, I. A. (1963) On the variation of radio star and satellite scintillation with zenith angle, *J. Atmos. Terr. Phys.* 25:339-366.

Table 1 lists the variety of experiments performed during 16-30 October 1976. The maximum latitude and longitude excursions of the 400-km subionospheric points during the period are also indicated.

Table 1. List of Stations and Experiments Performed During 16-30 October 1976

Station	Experiment	Frequency MHz	Satellite used, where applicable	400-km Ionospheric location explored
Jicamarca	Radar backscatter	50	-	11.97°S - 76.86°W
Ancon	Spaced receiver scintillation	249	LES-9	11.85°S - 8.33°S 73.92°W - 73.62°W
Huancayo	Scintillation	249	LES-9	12.07°S - 8.64°S 72.32°W - 72.03°W
	Scintillation	257 1541	MARISAT	11.09°S - 10.76°S 67.94°W - 67.69°W
		137	WIDEBAND	4°N - 26°S 61°W - 84°W
AFGL Aircraft	Scintillation ionosonde airglow	249	LES-9	10°S - 13°S 72°W - 76°W
AFAL Aircraft	Scintillation	249	LES-9	10°S - 13°S 72°W - 76°W

3. RELATIONSHIP BETWEEN IRREGULARITY PARAMETERS, SCINTILLATION INDEX, AND BACKSCATTERED POWER

3.1 Irregularity Parameters and Scintillation

The irregularities of electron density in the ionosphere impose phase fluctuations on a radio wavefront as it traverses an irregularity layer. Owing to phase mixing, amplitude fluctuations develop as the wave travels towards the ground. In the case of geostationary satellite observations, the satellite and the observer on ground are fixed relative to each other. However, owing to the superrotation of the ionosphere, the diffraction pattern on the ground sweeps past a fixed observing location and gives rise to fluctuations of the received signal power.

For an orbiting satellite, the ray path from the satellite to ground sweeps the ionospheric height at a speed of several kilometers per second. This speed is one to two orders of magnitude larger than the drift speed of the irregularities. As such, the irregularities may be considered to be frozen and the ground diffraction pattern sweeps past the observer owing to the motion of the satellite.

The quantitative measure of amplitude fluctuations is usually given by a scintillation index. The theory-based scintillation index (S_4) is defined as the normalized second central moment of the received signal power.¹⁹ For weak amplitude scintillations ($S_4 \leq 0.5$), a closed form solution providing the relationship between S_4 and the irregularity parameters, such as the electron density deviation and scale size, was initially developed under the assumption of a gaussian irregularity spectrum.¹⁹ Later, the satellite in situ measurements revealed that the F-region irregularities have a power law type of spectrum.⁸ Considering a power law irregularity power spectrum with a 3-dimensional spectral index of 4, in conformity with the in situ results, Rufenach²⁰ developed a relationship between the S_4 index and the irregularity parameters. Rufenach's equation introduced the effect of anisotropy of the irregularities in an ad hoc manner. Recently, Costa and Kelley²¹ introduced the anisotropy effect more rigorously in Rufenach's equation and obtained the following relationship:

$$S_4^2 = 2\phi_0^2 [1 - I_0 \left\{ \left(\frac{\beta^2 - 1}{2} \right) x \right\} \exp \left\{ - \frac{(\beta^2 + 1)}{2\beta^2} \right\} x] \quad (1)$$

$$\phi_0^2 = \frac{1}{\sqrt{2}} \pi (r_e \lambda)^2 \frac{\alpha}{\beta} (L \sec \chi) \frac{<(\Delta N)^2>}{k_0} \quad (2)$$

where

I_0 = modified Bessel function of zero order

α = axial ratio of field aligned irregularities

$\beta^2 = \cos^2 \psi + \alpha^2 \sin^2 \psi$

ψ = angle between the ray and the magnetic field

$x = \frac{2k_0^2}{k_f^2}$

k_0 = outer scale wave number

k_f = Fresnel wave number ($= \sqrt{\frac{4\pi}{\lambda z}}$)

λ = radio wavelength

z = mean distance between the observer and the irregularities

r_e = classical radius of electron ($= 2.8 \times 10^{-15}$ m)

L = irregularity layer thickness

20. Rufenach, C. L. (1975) Ionospheric scintillation by a random phase screen spectral approach, Radio Sci. **10**:155-165.
21. Costa, E., and Kelley, M. C. (1976) Calculations of equatorial scintillations at VHF and GHz frequencies based on a new model of the disturbed equatorial ionosphere, Geophys. Res. Lett. **3**:677-689.

χ = ionospheric zenith angle of the obliquely incident radio wavefront

$\langle(\Delta N)^2\rangle$ = mean square electron density deviation.

Equations (1) and (2) provide the desired relationship between the scintillation index, S_4 , and the irregularity parameters in the case of weak scattering ($S_4 \lesssim 0.5$). Both from the point of view of scintillation modeling, as well as theoretical considerations of irregularity generation, the rms electron density deviation (to be abbreviated as ΔN) is important. From a knowledge of S_4 , the ΔN parameter is obtained from Eqs. (1) and (2), provided realistic assumptions can be made regarding the layer thickness, L , and the outer scale wave number, k_o . The factor L signifies the thickness over which the irregularities may be assumed to be distributed undiminished in magnitude. The recent radar backscatter maps indicate that during nighttime the equatorial F-region irregularities extend from the bottom-side F region well into the topside to altitudes as high as 1000 km. However, the electron density deviation ΔN is found to decrease at high altitudes and L is found to be typically of the order of 200 km for fully developed irregularity structures. The in situ measurements of Dyson et al.⁸ showed that the outer scale wave number is less than 0.6 km^{-1} . Basu and Basu⁷ used the OGO-6 in situ measurements of ΔN near Ascension Island and demonstrated that it was possible to model the simultaneous scintillation measurements of the COMSAT group at 6 GHz from Ascension Island if the layer thickness of 200 km and outer scale dimension of 20 km (corresponding to a wave number $k_o = 0.31 \text{ km}^{-1}$) are assumed. The morphology of equatorial scintillations developed by Basu et al.⁹ on the basis of the in situ measurements of ΔN and the above mentioned values of L and k_o show a marked longitude variation of equatorial scintillations, in agreement with the ground station observations. These modeling efforts indicating that $L = 200 \text{ km}$ and $k_o = 0.31 \text{ km}^{-1}$ are justifiable assumptions. It should be mentioned here that the scintillation theories and modeling have been based on a monotonic power law type of irregularity spectrum. The in situ measurements indicate that although this type of spectrum is most commonly observed, instances of the nonmonotonic type with most of the spectral power concentrated around scale sizes of the order of 1 km are occasionally observed.⁸

Considering the most commonly observed form of irregularity power spectrum and assuming $k_o = 0.31 \text{ km}^{-1}$, we may utilize Eqs. (1) and (2) to obtain an estimate of electron density deviation ΔN for a given scintillation index. In the weak scatter limit of $S_4 = 0.5$ (corresponding to SI = 10 dB) and for the present geometry of LES-9 observations from Huancayo and Ancon, the above equation yields $\Delta N = 3 \times 10^{10} \text{ m}^{-3}$. Considering a typical value of ambient ionization density (N) as $6 \times 10^{11} \text{ m}^{-3}$, one obtains an irregularity amplitude ($\Delta N/N$) of 5 percent. For stronger scintillations, Eqs. (1) and (2) are not valid and an iterative method of

computation of S_4 is required.²² The foregoing discussion provides a fair idea of interpreting the observed scintillation measurements in terms of the irregularity parameter ΔN .

3.2 Irregularity Parameters and Radar Backscatter

Booker²³ developed the basic relationship between the irregularity power spectrum and the backscattering coefficient σ_B defined as the backscattered power per unit solid angle, per unit incident power density per unit volume as

$$\sigma_B = \frac{1}{(4\pi)^2} \cdot k^4 \left(\frac{f_p}{f}\right)^4 \left(\frac{\Delta N}{N}\right)^2 P(2k) \quad (3)$$

where

- f_p = plasma frequency of the ionized medium
- f = frequency of the incident wave
- k = wave number of the incident wave
- $\left(\frac{\Delta N}{N}\right)^2$ = mean square irregularity amplitude
- $P(2k)$ = power spectral density of irregularity wave number, $2k$.

Booker²³ obtained an expression for σ_B in the case of axially symmetric field-aligned irregularities described by a gaussian autocorrelation function. In view of the in situ results, Yeh et al²² assumed an isotropic power law type of irregularity power spectrum and derived the value of σ_B . Recently, Woodman and Basu²⁴ obtained an expression for the more realistic case of backscattered power from highly field-aligned irregularities having a power law type of irregularity spectrum. These authors show that the ratio of the backscattered power from irregularities (P_F) to the incoherent scatter power (P_i) is of the following form:

$$10 \log \frac{P_F}{P_i} = \frac{<(\Delta N)^2>}{N} \frac{8\pi^2 L_o^2}{[1 + k_{\perp}^2 L_o^2]^{3/2} \theta k_{\perp}} \quad (4)$$

22. Yeh, K. C., Liu, C. H., and Youakim, M. Y. (1975) A theoretical study of the ionospheric scintillation behavior caused by multiple scattering, Radio Sci. 10:97-106.
23. Booker, H. G. (1956) A theory of scattering by nonisotropic irregularities with application to radar reflections from the aurora, J. Atmos. Terr. Phys. 8:204-221.
24. Woodman, R. F., and Basu, Sunanda (1977) Comparison between in situ spectral measurements of equatorial F-region irregularities and backscatter observations at 3 m wavelength (abstract) EOS Trans. AGU 58:449.

where

- $\langle (\Delta N)^2 \rangle$ = mean square electron density fluctuations
- N = ambient ionization density
- L_o = outer scale size of the irregularity power spectrum
- θ = beam width of the radar antenna (0.7° for Jicamarca radar)
- k_\perp = 2 m^{-1} for 50-MHz radar.

The radar backscatter maps provide the left-hand side of Eq. (4), as discussed in Section 4. Thus, from a knowledge of N , L_o , k_\perp , and θ , $\langle (\Delta N)^2 \rangle$ may be obtained. Woodman and Basu²⁴ obtained estimates of $\langle (\Delta N)^2 \rangle$ from scintillation measurements by using Eqs. (1) and (2) and substituted that value in Eq. (4) to obtain the intensity of the backscattered power. Their results indicate a large discrepancy of four orders of magnitude between the observed and computed intensity levels. They have related the discrepancy to the possible existence of a cutoff in the irregularity power spectrum near the ion gyro-radius which is typically of the order of 3 m at F-region heights.

4. RESULTS

Ground scintillation measurements were performed on all days covering the period 16-30 October 1976. The Jicamarca radar was, however, operated on only seven nights during this period. The simultaneous radar and scintillation observations made on these seven nights are discussed below in a chronological manner. Nighttime scintillations in the equatorial region are observed between 1900 and 0100 local time. In the present set of illustrations, the radar maps indicate both local time, referred to the 75° W meridian, and universal time, whereas the scintillation data are plotted against universal time only.

4.1 Observations Made on 16-17 October 1976

Figure 2(a) shows the digital power map acquired at Jicamarca by the use of the 50-MHz radar backscatter experiment. The maps exhibit the range of the scattering region, as well as the backscattered power as a function of time. The original digital maps provide the backscattered power relative to the approximate maximum incoherent scatter level in the range between 6 dB and 48 dB at 6-dB intervals. As the original digital maps are difficult to reproduce, they have been redrawn to depict only four ranges of relative power levels. It has been mentioned earlier that the backscattered power at 50 MHz is caused by irregularities with scale lengths of 3 m. As such, these maps give the temporal variation of the 3-m irregularity

structures over Jicamarca. As noted by Woodman and La Hoz,¹² the digital power maps may be viewed as an east-west and vertical scan of the spatial irregularity configuration under the assumption of a rigid transport of irregularity structures with an average eastward drift speed of 125 m per sec.

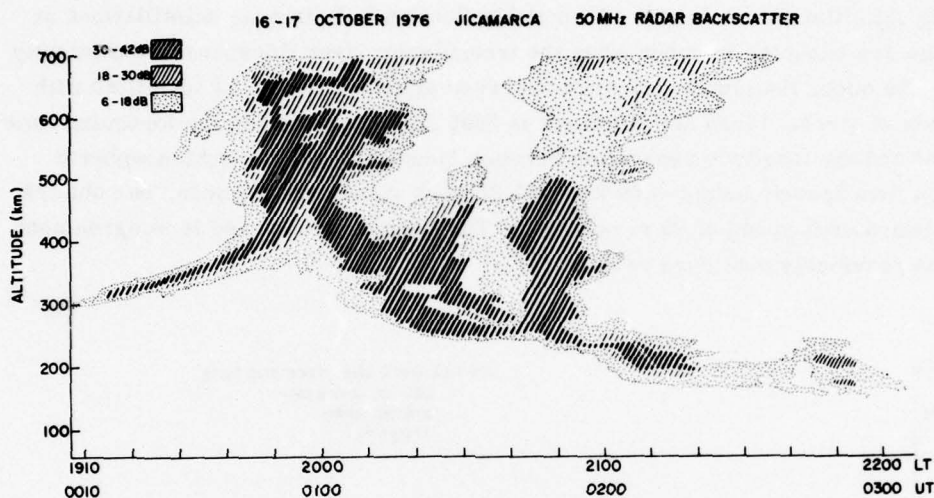


Figure 2(a). The 50-MHz Radar Backscattered Power Map of Nighttime Irregularities Obtained at Jicamarca on 16-17 October 1976

The radar map shown in Figure 2(a) indicates that on 16-17 October 1976, weak 3-m irregularities were first observed at 1910 LT at an altitude of 300 m. During the following half-hour interval, the minimum altitude of the irregularity layer increased from 300 to 400 km and the layer thickness increased to about 50 km. If we consider that the observed temporal variation was a result of a rigid transport of the irregularities at a drift speed of 125 m per sec, this portion of the digital map signifies a height variation of the minimum altitude of the irregularity layer. A 100-km increase in altitude for the bottom edge of the irregularity layer occurs over an east-west distance of only 225 km.

After 1945 LT, an extended irregularity structure, commonly referred to as a plume, is found to evolve. From a study of the backscattered power levels within the plume, it is concluded that very intense 3-m irregularities were present. The plume structure extended from an altitude of 400 km to 700 km; the existence of top-side irregularities connected to the bottomside may be noted. The plume structure ended at 2010 LT and during the following half-hour interval, an intense irregularity

layer of about 200-km thickness at low altitudes was detected. After 2040 LT, another plume with a duration smaller than the first plume structure evolved. Between the entire time interval of 2010 and 2110 LT, there occurred a gradual decrease of the minimum altitude of the irregularity region from 400 to 200 km.

Figure 2(b) illustrates the results of scintillation measurements made at Ancon by the use of 249-MHz transmissions from the LES-9 satellite. A comparison of Figures 2(a) and 2(b) indicates that the development of 3-m irregularities over Jicamarca preceded the onset of scintillations at Ancon, situated to the east of Jicamarca. It is likely that the irregularity structure observed over Jicamarca drifted eastwards causing scintillations at Ancon. As noted in Section 3.1, intense scintillations at 249 MHz are expected to occur when the irregularity layer thickness is sufficiently large. As such, the plume structure observed at 1950 LT is to be identified with the onset of strong Ancon scintillations at 2050 LT. Considering the foregoing time interval and the longitude separation between Jicamarca and the subionospheric location (ionospheric height—400 km) of LES-9 as viewed from Ancon, one obtains an eastward drift speed of 95 m per sec. The derived drift speed is in agreement with the previously published results.²⁵

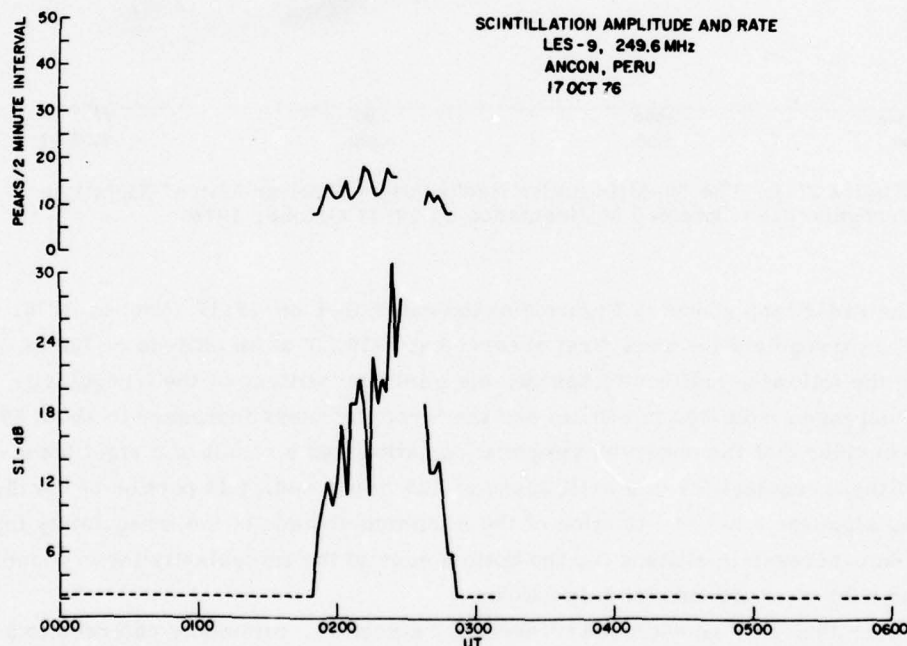


Figure 2(b). Temporal Variation of 249-MHz Scintillation Index, SI(dB), and Fading Rate Recorded on 16-17 October 1976, at Ancon on the Propagation Path to LES-9

25. Woodman, R. F. (1972) East-west ionospheric drifts at the magnetic equator, Space Research XII, Akademie-Verlag, Berlin, pp 968-974.

From the top panel of Figure 2(b), it is found that the fading rate is about 6 per minute. From the geometry of observations, the Fresnel zone radius is about 900 m. With the prevailing drift speed of 95 m per sec, the fading rate is expected to be 6 per min in the case of weak scattering. The observations indicate that the fading rate was 6 per min even though the scintillation index was as high as 30 dB, corresponding to the multiple scatter regime. In the case of multiple scattering, small scale diffraction patterns are expected to develop, giving rise to faster fading rates than obtained under weak conditions.^{21, 26} The slow fading rates observed in conjunction with high scintillation levels is an unexpected result. It may be mentioned that Woodman and La Hoz¹² reported the existence of large vertical velocities within an irregularity layer. Since the propagation paths for scintillation measurements were inclined towards the east, the component of vertical velocity of irregularities perpendicular to the propagation path will be oriented towards the west. This will reduce the effective eastward drift speed of individual irregularities and may give rise to the observed slow fading rates.

Figure 2(c) illustrates the results of scintillation measurements made at Huancayo with the 249-MHz transmissions from the LES-9 satellite. The bottom panel of the figure shows that a weak scintillation structure was initially observed, but after 2115 LT an intense scintillation structure similar to that obtained at Ancon was detected. The weak initial structure has, however, no counterpart in Ancon data; it is attributed to a weak irregularity patch developing between Ancon and Huancayo. The major scintillation structure of Huancayo commenced at 2116 LT and was delayed from the onset of Ancon scintillation by 26 minutes. This is consistent with an eastward drift of the irregularity patch from Ancon to Huancayo at a speed of 116 m per sec.

Thus a comparison of the radar map obtained at Jicamarca and scintillation observations of Ancon and Huancayo, illustrated in Figures 2(a), (b), and (c), shows that an irregularity patch evolving either at or to the west of Jicamarca, drifted eastwards at an approximate speed of 100 m per sec, causing the successive onsets of scintillation at Ancon and Huancayo. The duration of scintillation at either station was about 60 min which, on the basis of the average drift speed (100 m per sec), yields the E-W dimension of the patch as 360 km. The compatibility of radar and scintillation measurements on this night indicates that kilometer-sized irregularities causing scintillations co-existed with the 3-m irregularities giving rise to radar backscatter.²⁷ Considering the time interval between the onset of the plume structure at Jicamarca and the decay of scintillation at the easternmost location of Huancayo, one finds that the total lifetime of the irregularity patch is at least 2-1/2 hours.

26. Prokhorov, A. M., Bunkin, F. V., Gochilashvily, K. S., and Shishov, V. I. (1975) Laser irradiance propagation in turbulent media, *Proc. IEEE* 63:790-811.

27. Aarons, J., Buchau, J., Basu, Santimay, and McClure, J. P. (1978) The localized origin of equatorial F-region irregularity patches, *J. Geophys. Res.* (to be published).

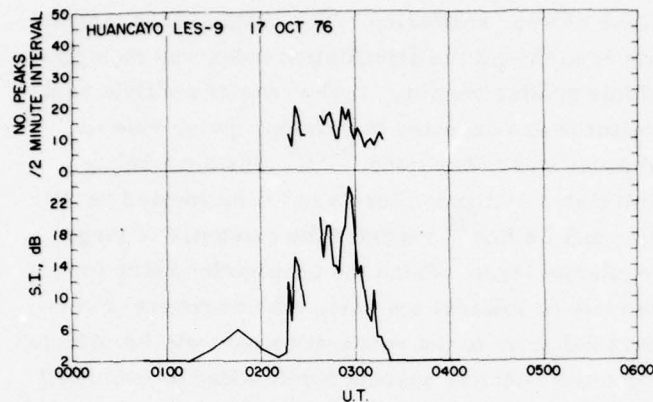


Figure 2(c). Temporal Variation of 249-MHz Scintillation Index, SI(dB), and Fading Rate Recorded on 16-17 October 1976, at Huancayo on the Propagation Path to LES-9

4.2 Observations Made on 18-19 October 1976

The results of simultaneous radar and scintillation measurements obtained on this night are shown in Figures 3(a), (b), (c), and (d). In order to retain the clarity of the radar map, it has been reproduced in two successive diagrams, Figures 3(a)-1 and 3(a)-2 with overlapping time scales. Figure 3(a) shows that when the radar started its operation at 1930 LT, a weak and thin layer of 3-m irregularities had already evolved at an altitude of about 200 km. The radar data was, unfortunately, interrupted between 2050 and 2123, making it difficult to ascertain the nature of irregularity structure during this time period. However, a closer examination of the bottomside structures seen around 2050 LT and the topside structures prior to 2130 LT indicates that a plume structure evolved shortly after 2050 LT. The structure decayed after 2200 LT and patchy irregularities extending over several hundred kilometers existed until 2340 LT. In the following discussion, we shall consider that, on this night, an extended plume structure occurred over Jicamarca at 2100 LT.

From the bottom panels of Figures 3(b) and 3(c) we find that both ground stations, Ancon and Huancayo, observed two scintillation structures, the first structure having a duration of about 1-1/2 hour at both stations and the second having a 3 hour duration at Ancon and 2 hours only at Huancayo. The wide second structure shows the existence of a large number of substructures. A comparison of Figures 3(a), 3(b), and 3(c) indicates that there is no correspondence between the radar map and the first scintillation structure observed at Ancon and Huancayo. Although there is an initial interruption in the scintillation data acquired at Ancon, there can be no question regarding the commencement of scintillations nearly an hour before the onset of plume structures over Jicamarca. This may signify two possibilities: (1) To assume that an irregularity structure developed between Ancon and Jicamarca so that it was not possible for the radar to detect it; (2) to assume that the

irregularity patch had most of its spectral power at kilometer wavelengths and negligible power at 3-m wavelength. Thus when the irregularity structure made its transit over Jicamarca, it could not be detected by the radar, but when it drifted to the subionospheric locations of scintillation measurements it gave rise to intense scintillations. The in situ results⁸ have shown that in certain exceptional cases, nighttime equatorial irregularities may have most of the spectral power around a scale size of 1 km.

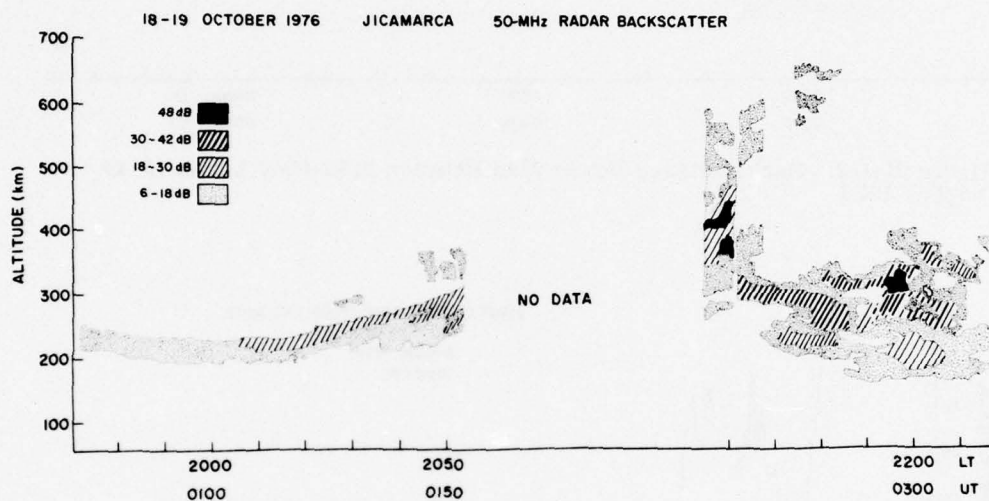


Figure 3(a)-1. Radar Backscattered Power Map Recorded at Jicamarca Between 1930-2210 LT on 18-19 October 1976

18-19 OCTOBER 1976 JICAMARCA 50-MHz RADAR BACKSCATTER

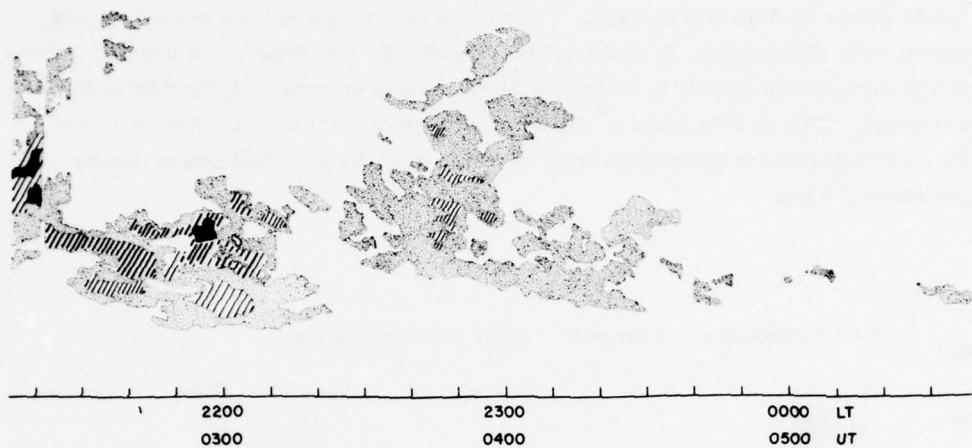


Figure 3(a)-2. Backscattered Power Map Between 2120-0040 LT on 18-19 October 1976

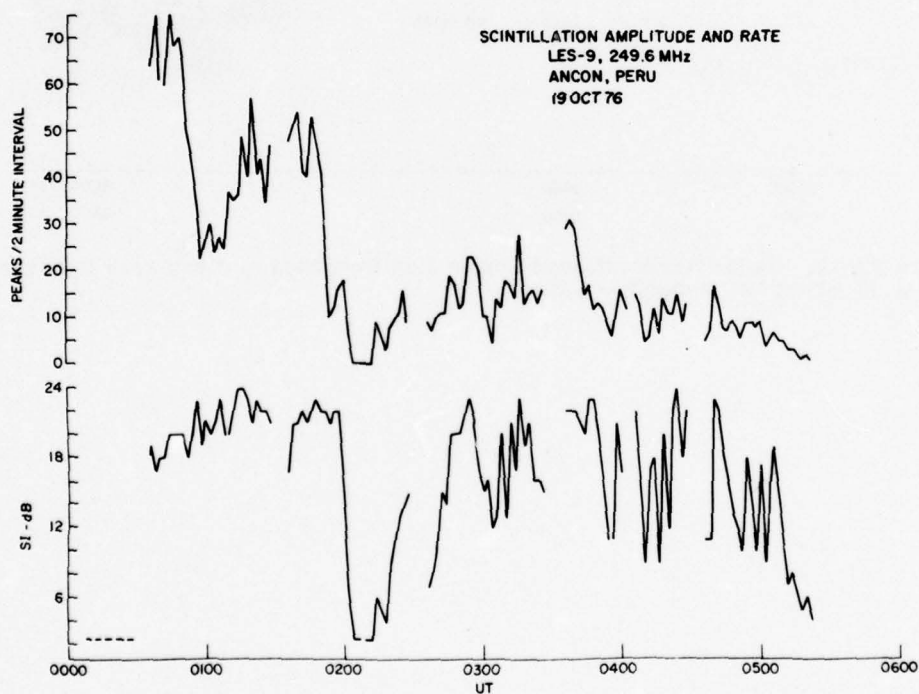


Figure 3(b). Temporal Variation of 249-MHz Scintillation Index, SI(dB) and Fading Rate Recorded at Ancon by the Use of LES-9 Satellite on 18-19 October 1976

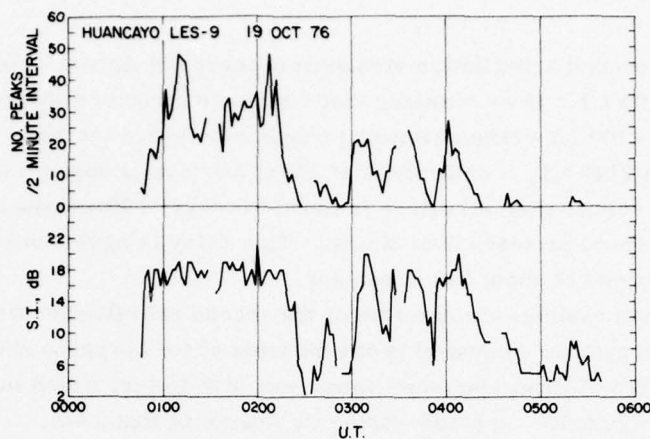


Figure 3(c). Temporal Variation of 249-MHz Scintillation Index, SI(dB) and Fading Rate Recorded at Huancayo by the Use of LES-9 Satellite on 18-19 October 1976

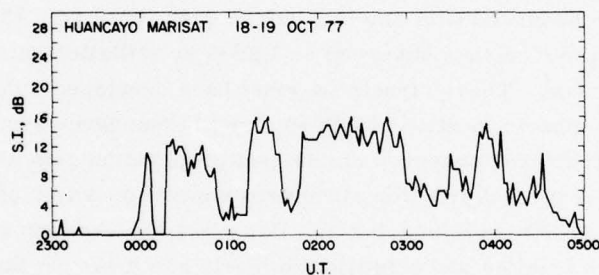


Figure 3(d). Temporal Variation of 257-MHz Scintillation Index, SI(dB) Recorded at Huancayo with Marisat Satellite on 18-19 October 1976

In view of the Ancon data interruption at the outset, we compare the time interval between the decay of scintillations at Ancon and Huancayo for the first structure in order to derive the drift speed of the patch. We find that the decay at Huancayo was delayed by about 25 min, consistent with an eastward drift of the irregularity patch at a speed of 116 m per second. Combining this drift speed with the duration of scintillations at Huancayo, one observes that the E-W dimension of the irregularity patch is about 700 km. From the top panels of Figures 3(b) and 3(c), high fading rates may be noted. The Ancon data, in particular, indicate fading rates as large as 30 per min. As mentioned earlier, such high fading rates are expected under multiple scatter conditions.

The broad second scintillation structure observed at Ancon commenced gradually at about 2120 LT. If we consider that the plume structure observed over Jicamarca at about 2100 LT drifted eastward causing the sharp increase of Ancon scintillations at 2140 LT, a drift speed of 140 m per sec is observed. The corresponding part of scintillation structure is found to occur at Huancayo after a delay of 20 min from its occurrence over Ancon. This delay is again consistent with an eastward drift speed of about 140 m per sec.

As mentioned earlier, the duration of the second scintillation structure was shorter at Huancayo, as compared to the duration of the corresponding event at Ancon. The depth of Huancayo scintillation was also lower, which may signify the decay of the irregularity structure during its transit to Huancayo.

On this night, scintillation measurements were also made at Huancayo with the 257-MHz transmissions from Marisat. From Figure 1, it may be noted that the intersection of the propagation path from Huancayo to Marisat explored the easternmost location of the ionosphere for the present set of observations; it was located 350 km to the east of the subionospheric point of LES-9, as observed from Huancayo. The temporal variation of Marisat scintillation is shown in Figure 3(d). The scintillation structures observed with Marisat before 0142 (2042 LT, 75° W time) cannot be identified with any structure observed on LES-9 scintillation data acquired at Huancayo, or at Ancon. These structures must have developed independently to the east of the subionospheric location of LES-9 viewed from Huancayo. The remaining two scintillation structures observed on Marisat propagation path after 0142 UT seem to correspond to the two scintillation structures observed earlier on the propagation paths from LES-9 to Huancayo and Ancon. However, the duration of these two events is found to be much smaller and scintillation levels are lower on Marisat propagation paths, as compared to the corresponding features on LES-9 propagation paths. It is not possible to conclude definitely whether the irregularity structures observed on the propagation paths of LES-9 to Ancon and Huancayo decayed both in strength and extent during their eastward travel over a distance of about 700 km, or if the propagation path to Marisat was encountering independent irregularity structures. The former is more likely, as the decay of the structures could be noted during their passage between the subionospheric positions of LES-9 viewed from Ancon and Huancayo.

4.3 Observations Made on 19-20 October 1976

Figures 4(a), (b), (c), (d), and (e) illustrate the results of radar and scintillation measurements obtained on this night. The radar map shows that at Jicamarca two well-separated plume structures were observed, the first plume being much wider than the second. The scintillation measurements indicate that Huancayo,

situated to the east of Ancon, observed five scintillation structures, whereas Ancon recorded four scintillation patches.

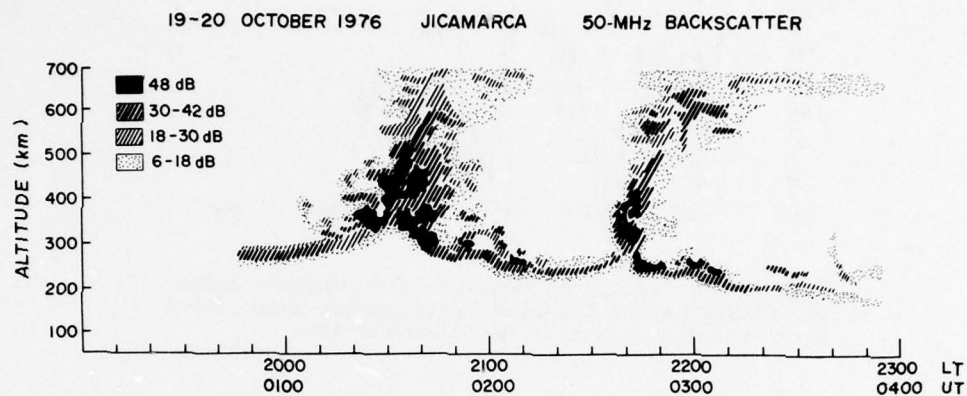


Figure 4(a). Radar Backscattered Power Map Obtained at Jicamarca on 19-20 October 1976

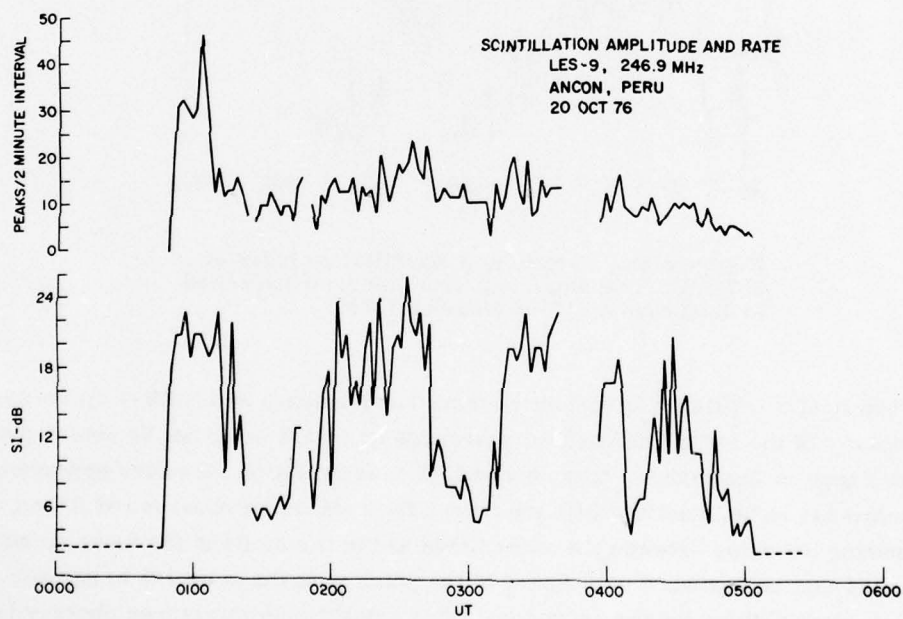


Figure 4(b). Temporal Variation of Scintillation Index and Fading Rate of 249-MHz Transmissions from LES-9 Recorded at Ancon on 19-20 October 1976

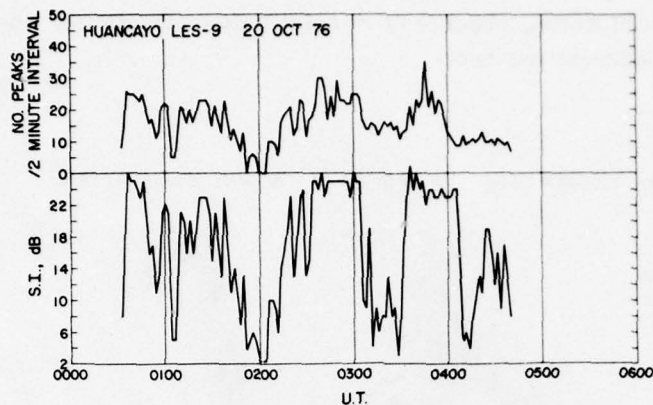


Figure 4(c). Temporal Variation of Scintillation Index and Fading Rate of 249-MHz Transmission from LES-9 Recorded at Huancayo on 19-20 October 1976

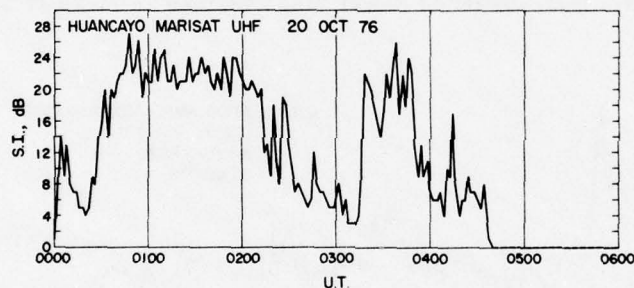


Figure 4(d). Variation of Scintillation Index of 257-MHz Transmissions from Marisat Recorded at Huancayo on 19-20 October 1976

The first scintillation structure observed at Huancayo with LES-9 evolved in the vicinity of the station and drifted eastwards so that it could not be detected at either Ancon or Jicamarca. The second LES-9 scintillation structure observed at Huancayo has to be identified with the first LES-9 structure observed at Ancon. Comparing the delay between the onset times at the two stations for these structures, one notes that an eastward drift speed of the patch is found to be 125 m per sec. Similar computations for the second and third scintillation structures observed over Ancon provide eastward drift speeds ranging between 120 and 130 m per sec. The fourth scintillation structures observed at Ancon and the corresponding (fifth) structure at Huancayo are found to commence simultaneously. It seems that the two

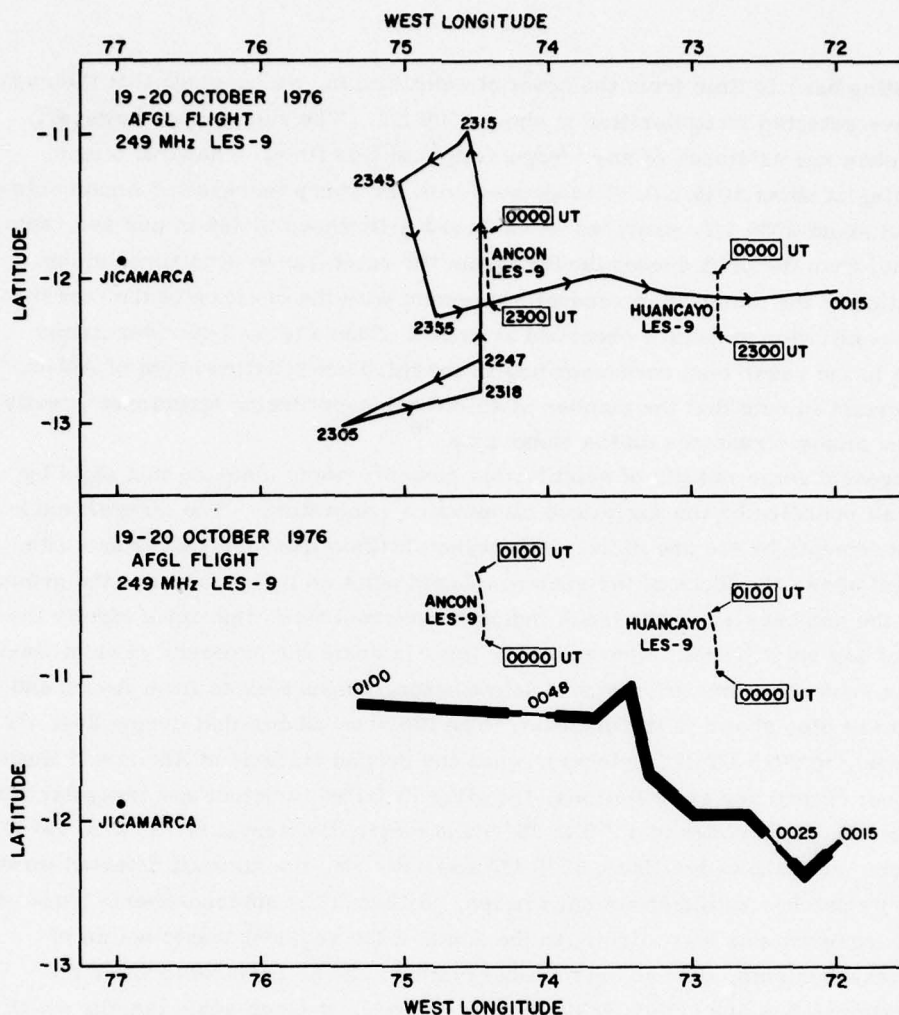


Figure 4(e). Subionospheric Flight Path of the AFGL Aircraft Making 249-MHz Scintillation Observations with LES-9 on 19-20 October 1976. Thin and thick lines indicate respectively the absence or presence of scintillations

stations were observing two independent irregularity structures. While there is good correspondence between the scintillation structures observed with LES-9 at the two ground stations, the results of Marisat observations illustrated in Figure 4(d) indicate that this propagation path was encountering independent structures.

If we now concentrate on the radar map shown in Figure 4(a), we find that the first plume developed at about 2015 LT. Let us consider that the first scintillation event observed at Ancon (1945 LT) was generated by an irregularity structure drifting eastwards from Jicamarca. Assuming a drift speed of 120 m per sec and

extrapolating back in time from the onset of scintillation, we conclude that the radar should have detected irregularities at about 1900 LT. The radar map, however, does not show the existence of any irregularities at this time. The first plume commencing at about 2015 LT, if associated with the sharp increase of Ancon scintillation at about 2055 LT, provides an eastward drift speed of 140 m per sec, somewhat higher than the drift speeds derived from the scintillation structures alone. The duration of the plume is in general agreement with the duration of the corresponding scintillation structure observed at Ancon. There is no 3-m irregularity structure in the radar map corresponding to the third scintillation event of Ancon. It is important to note that the number of scintillation-producing structures greatly exceed the plume structures on the radar map.²⁸

We present some results of scintillation measurements made on this night by the aircraft operated by the Air Force Geophysics Laboratory. The aircraft made the measurements by the use of 249-MHz transmissions from the LES-9 satellite. Figure 4(e) shows the locus of the subionospheric point as it flew between the ground stations; the numbers along the track indicate universal time; thin lines signify the absence of any scintillation, whereas thick lines indicate the presence of scintillation. The subionospheric positions of scintillation measurements from Ancon and Huancayo are also shown in the diagram. The top panel shows that during 2247 UT (19 October), to 0015 UT (20 October), when the ground stations at Ancon and Huancayo did not record any scintillations, the aircraft failed to detect any irregularities in the entire latitude range of 11° S to 13° S and longitude interval of 72° W to 75° W. The bottom panel shows that from 0015 UT and onwards, the aircraft detected three irregularity patches with distinct boundaries. Although the subionospheric track of aircraft measurements was slightly to the south of the subionospheric points of ground measurements, the two sets of observations can be correlated since the irregularity patches are highly field-aligned, at least, at large scale lengths which cause scintillations. The first patch observed between 0015 and 0025 UT was situated to the east of Huancayo. The structure observed between 0025 and 0048 UT provide the E-W extent of the irregularity structure, causing the first scintillation activity observed at Huancayo. The westward termination of the patch was to the east of Ancon and, therefore, the Ancon ground station did not record any scintillation from this patch. The patch located between 0048 to 0100 UT caused the first scintillation structure observed at Ancon. This patch subsequently drifted eastwards, causing the second scintillation event at Huancayo. It may be of interest to mention that at about 0050 UT while the aircraft was traveling due west in the vicinity of

28. Basu, Santimay, Aarons, J., McClure, J. P., and Calderon, C. (1977) Combined study of nighttime equatorial irregularities by radar backscatter, ground-based and airborne scintillation measurements (abstract), EOS Trans. AGU 58:450.

Ancon, the fading rate of scintillations recorded on the aircraft was 30 fades per min, whereas Figure 4(b) shows that at this time the fading rate of ground station (Ancon) scintillation measurement was only 15 fades per min. The average eastward drift speed of the irregularity patch has been shown to be 120 m per sec and owing to the motion of the aircraft, the subionospheric point was drifting westward at about the same speed, giving rise to an increase in the aircraft scintillation fading rate by a factor of 2.

4.4 Observations Made on 20-21 October 1976

Figures 5(a)-1 and 5(a)-2 show the radar map obtained at Jicamarca. We observe that on this night the radar could detect only weak bottomsides irregularities in a thin layer. On this night no scintillations were observed at either Ancon or Huancayo with LES-9 or Marisat, signifying the absence of any irregularities over an E-W distance of about 800 km. As indicated in Section 3.1, weak and thin irregularity layers are not expected to cause VHF-UHF scintillations. It may be quite likely that the radar did not detect any irregularities that night but merely registered partial reflections from steep gradients of the ionization profile.²⁹

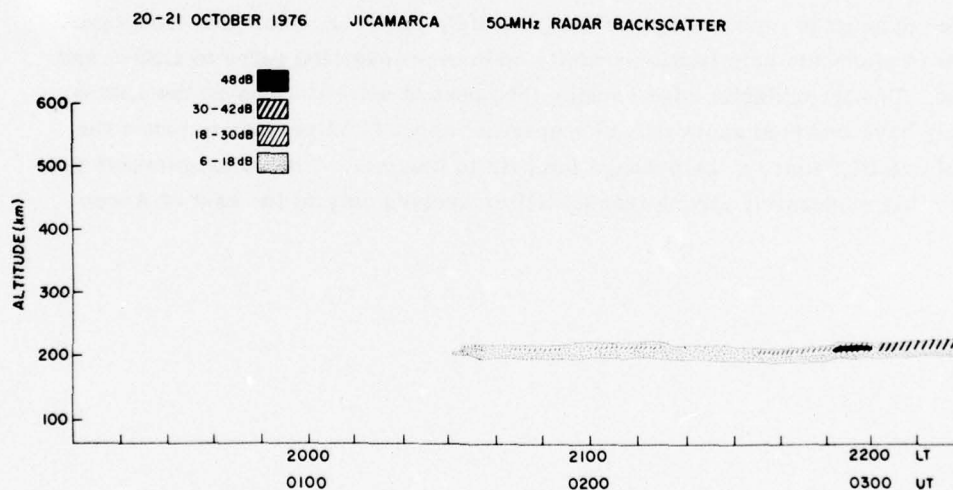


Figure 5(a)-1. Backscattered Power Map Obtained at Jicamarca Between 1910-2220 LT on 20-21 October 1976

29. Balsley, B.B., and Farley, D.T. (1975) Partial reflections: A source of weak VHF equatorial spread-F echoes, J. Geophys. Res. 80:4735-4737.

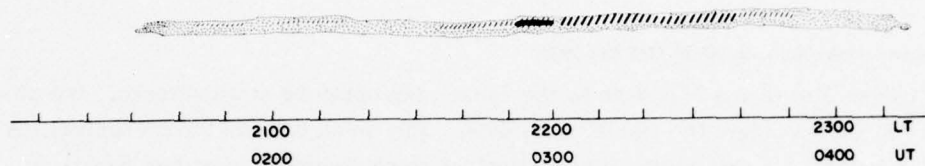


Figure 5(a)-2. Backscattered Power Map Between 2050-2320 LT on 20-21 October 1976

4.5 Observations Made on 21-22 October 1976

Also on this night, the radar could detect only weak bottomside irregularities as shown in Figures 6(a)-1 and 6(a)-2. Figure 6(b) shows that at Ancon, except for a few brief periods of 3-6 dB scintillation, no significant scintillation event was observed during the night. Figures 6(c) and 6(d), however, show that Huancayo registered moderate scintillation activity on both propagation paths to LES-9 and Marisat. The irregularity edge causing the onset of scintillations on the LES-9 path may have traveled eastwards at a speed of about 85 m per sec to cause the onset of scintillations on the propagation path to Marisat. The measurements thus indicate that moderately strong irregularities evolved only to the east of Ancon.

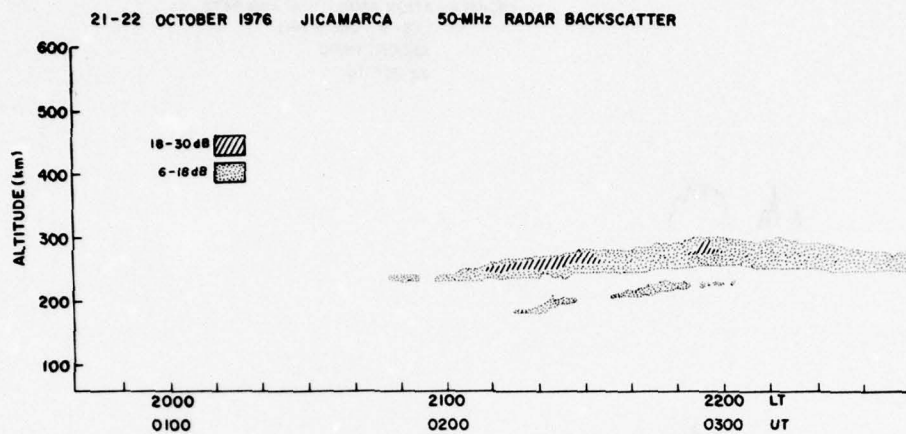


Figure 6(a)-1. Backscattered Power Map Obtained at Jicamarca Between 1940-2240 LT on 21-22 October 1976

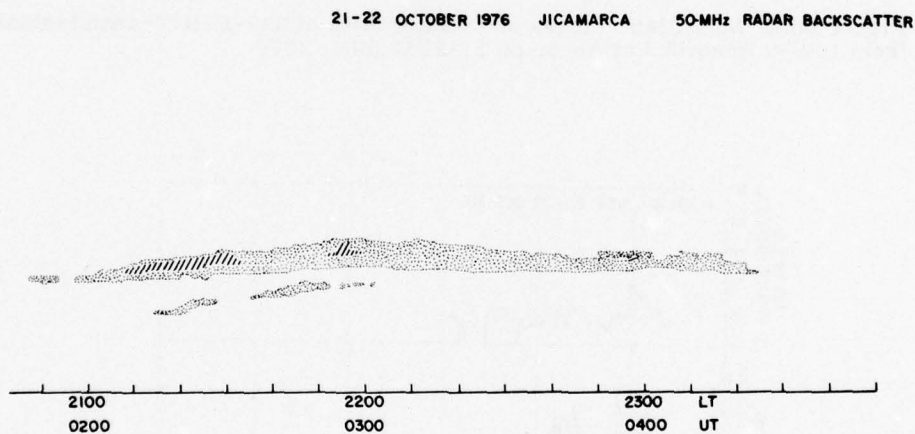


Figure 6(a)-2. Backscattered Power Map Between 2050-2350 LT on 21-22 October 1976

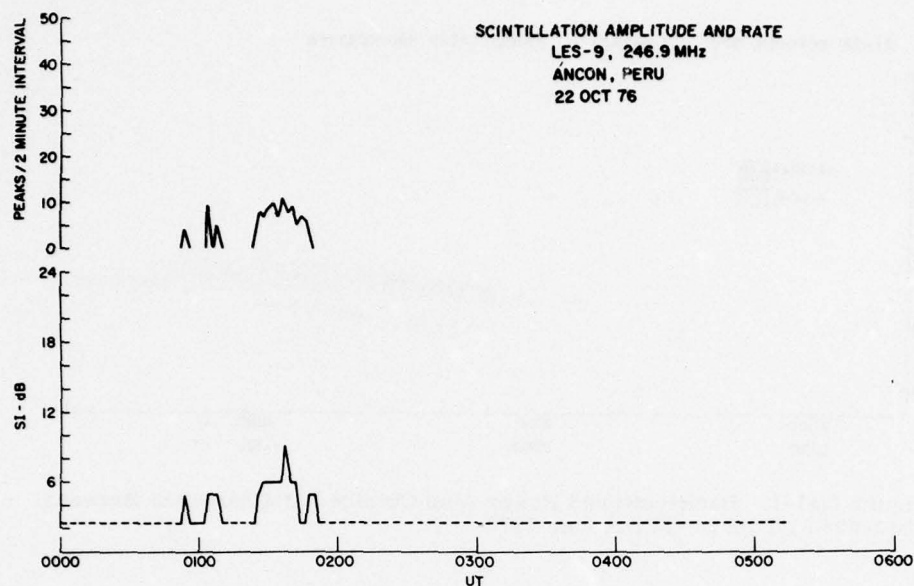


Figure 6(b). Scintillation Index and Fading Rate of 249-MHz Transmissions from LES-9 Recorded at Ancon on 21-22 October 1976

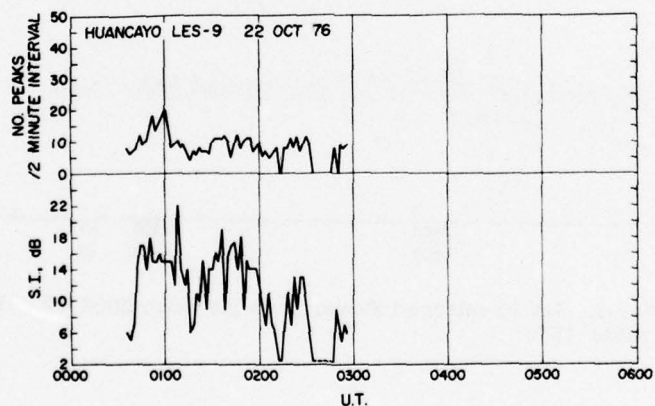


Figure 6(c). Scintillation Index and Fading Rate of 249-MHz LES-9 Transmissions Recorded at Huancayo on 21-22 October 1976

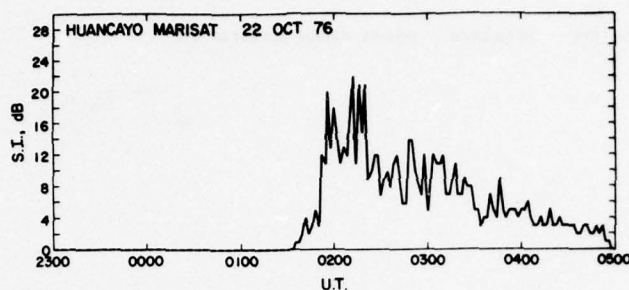


Figure 6(d). Scintillation Index of Marisat Transmissions at 257 MHz Recorded at Huancayo on 21-22 October 1976

4.6 Observations Made on 24-25 October 1976

The radar map of 3-m irregularities obtained on this night is illustrated in three successive Figures 7(a)-1, 7(a)-2, and 7(a)-3 with overlapping time scales. The conspicuous feature of the map is the development of a rather thick and strong irregularity layer after local midnight, whereas during the premidnight hours mostly weak irregularities were observed. The Ancon scintillation observations shown in Figure 7(b) were interrupted after 0315 UT, making it difficult to compare the radar map. At Huancayo, however, scintillation measurements with LES-9 were not interrupted and two distinct events were recorded. Both structures were observed prior to the local midnight and possibly correspond to the two partial structures recorded at Ancon. Corresponding to these scintillation events, no conspicuous feature on the radar map is discernible. On the other hand, the postmidnight 3-m irregularity structure observed by the radar does not have any corresponding scintillation event at Huancayo. Unfortunately, the Ancon data were interrupted during this period, and it is not clear if this irregularity structure decayed during its transit to Huancayo at a distance of 500 km to the east.

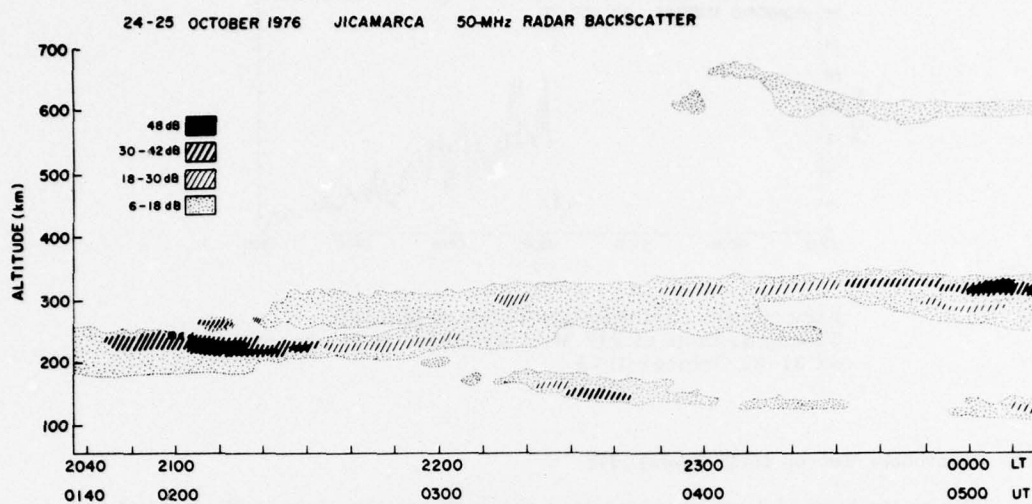


Figure 7(a)-1. Backscattered Power Map Obtained at Jicamarca Between 2040-0010 UT on 24-25 October 1976

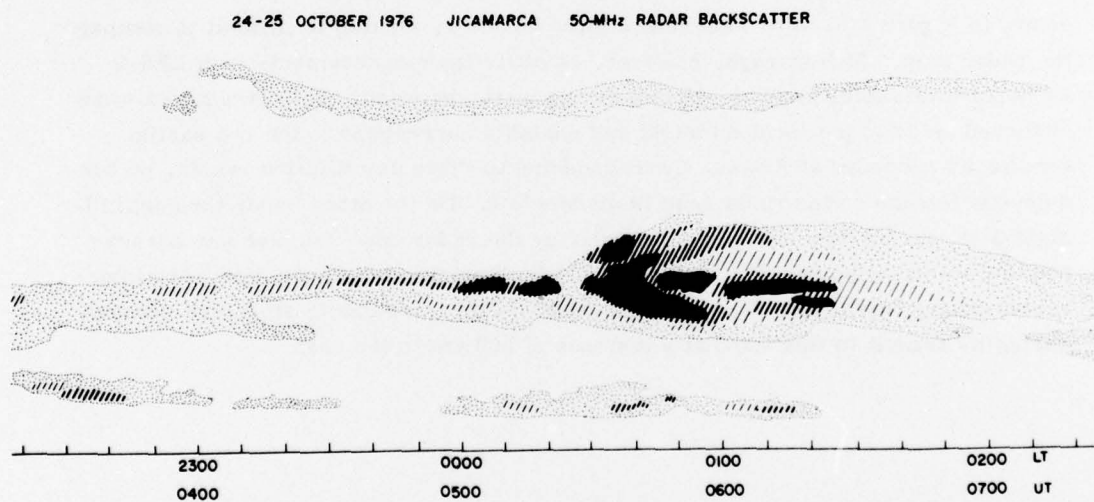


Figure 7(a)-2. Backscattered Power Map Between 2220-0220 LT on 24-25 October 1976

24-25 OCTOBER 1976 JICAMARCA 50-MHz RADAR BACKSCATTER

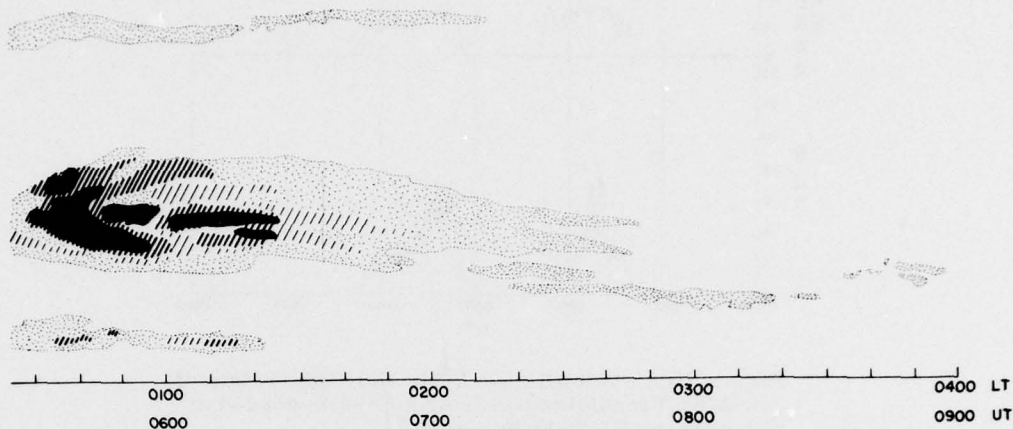


Figure 7(a)-3. Backscattered Power Map Between 0030-0400 LT on 24-25 October 1976

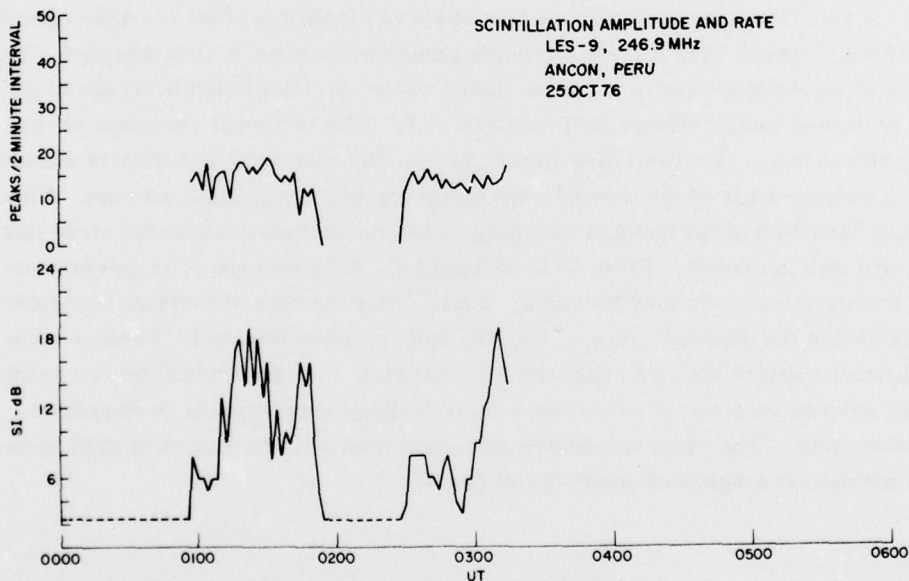


Figure 7(b). Scintillation Index and Fading Rate of 249-MHz Transmissions from LES-9 Recorded at Ancon on 24-25 October 1976

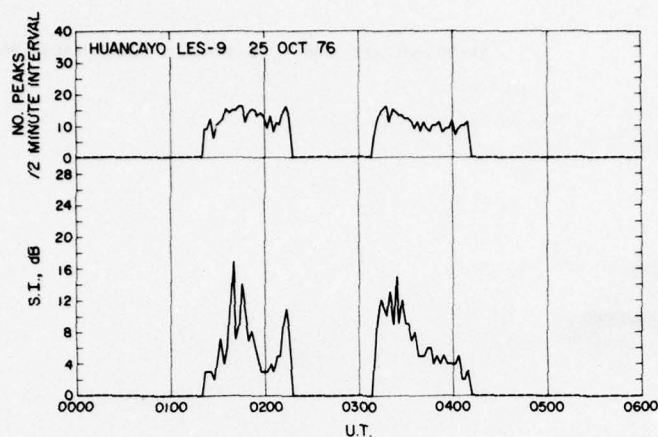


Figure 7(c). Scintillation Index and Fading Rate of 249-MHz Transmissions from LES-9 Recorded at Huancayo on 24-25 October 1976

4.7 Observations Made on 29-30 October 1976

Figure 8(a)-1, 8(a)-2, and 8(a)-3 illustrate the radar backscatter map for this night. A thin irregularity structure was observed from the start of radar operation at 1930 LT to about 2010 LT when topside irregularities were also detected. These topside irregularities are found to be linked to the thick bottomside irregularity layer observed later between 2050 and 2115 LT. The temporal variation of the irregularity location observed over Jicamarca during this period of time is consistent with an eastward tilt of the irregularity structure with increasing altitude. This is the only case during the October campaign when an eastward tilt of the irregularity structure was observed. From 2115 to 2200 LT, the presence of an intense and thick irregularity layer may be noted. Later, only patches of isolated irregularities distributed in the altitude range of 200 and 600 km were detected. From a study of scintillation results shown in Figures 8(b) and 8(c), it is found that the two scintillation structures detected at Ancon have their delayed counterparts in Huancayo measurements. The observed delays are consistent with an eastward drift speed of these patches at a speed of about 100 m per sec.

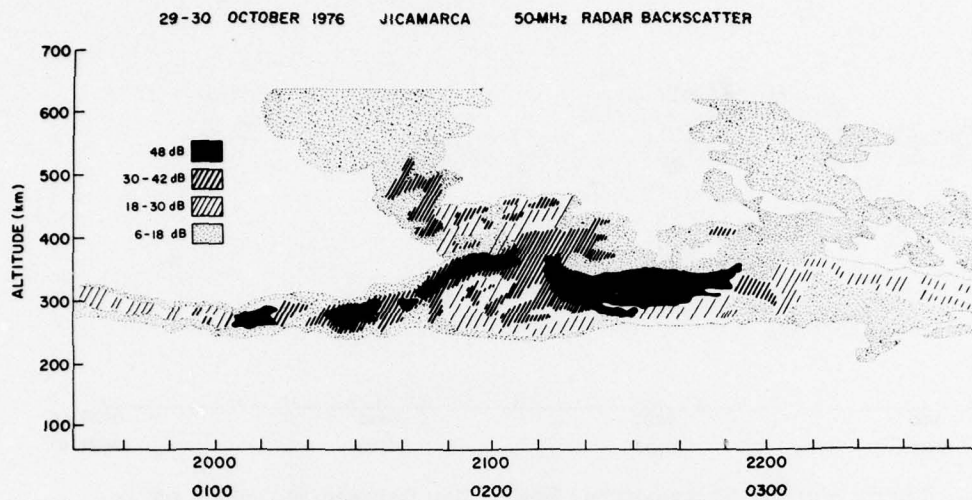


Figure 8(a)-1. Backscattered Power Map Obtained at Jicamarca Between 1930-2240 LT on 29-30 October 1976

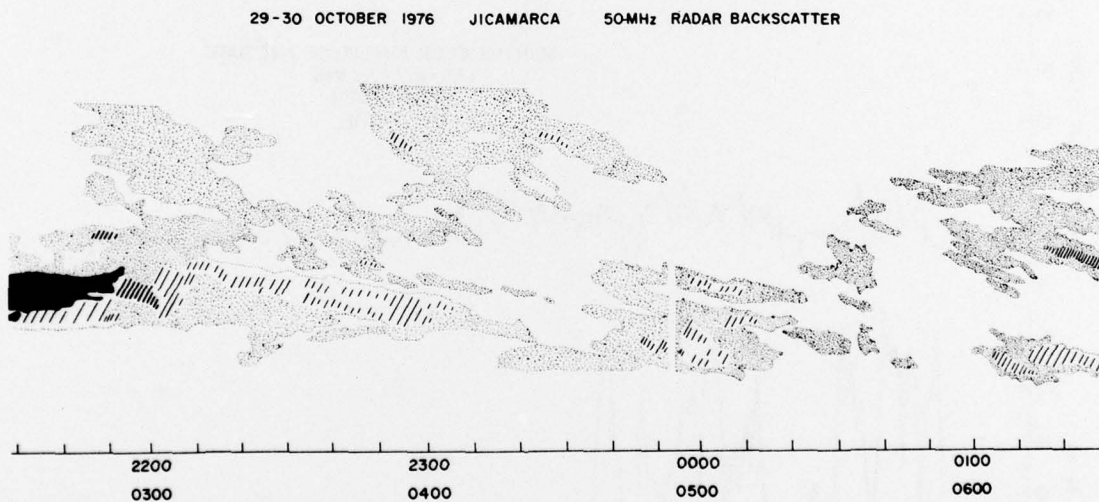


Figure 8(a)-2. Backscattered Power Map Between 2130-0120 LT on 29-30 October 1976

29-30 OCTOBER 1976 JICAMARCA 50-MHz RADAR BACKSCATTER

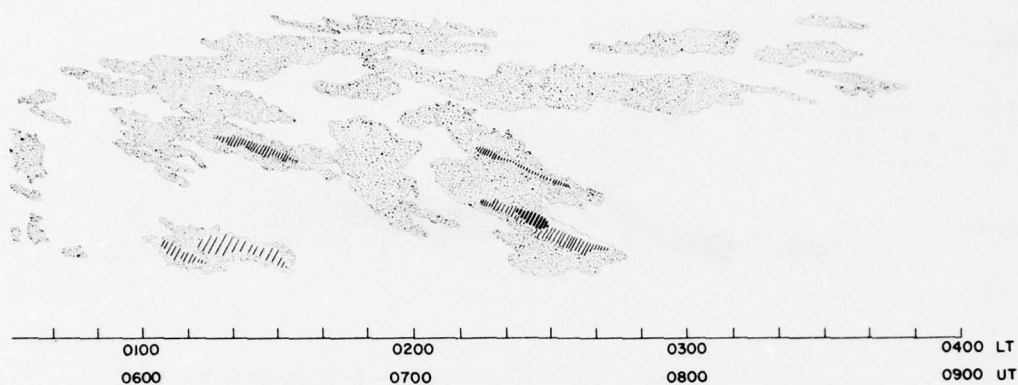


Figure 8(a)-3. Backscattered Power Map Between 0040-0400 LT on 29-30 October 1976

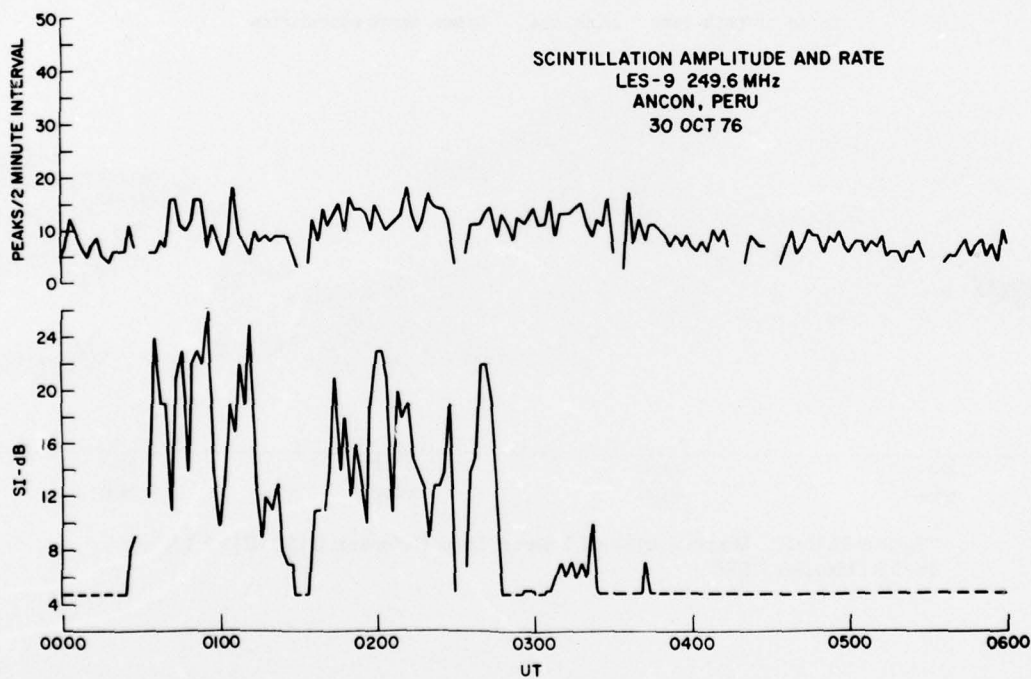


Figure 8(b). Scintillation Index and Fading Rate of 249-MHz Transmissions from LES-9 Recorded at Ancon on 29-30 October 1976

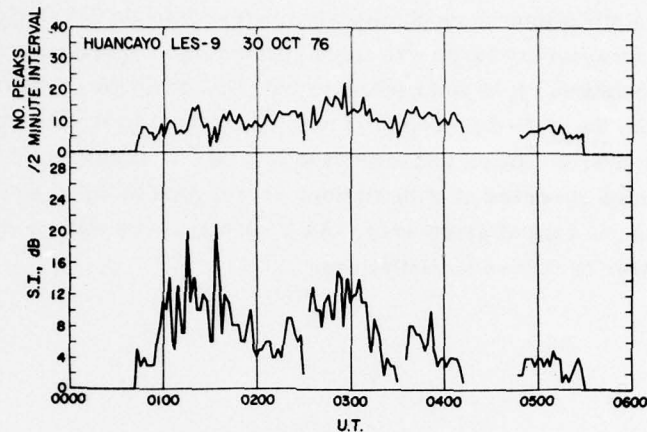


Figure 8(c). Scintillation Index and Fading Rate of 249-MHz Transmissions from LES-9 Recorded at Huancayo on 29-30 October 1976

However, the first scintillation structure at Ancon cannot be associated with any feature on the radar map; it has to be viewed as an independent irregularity structure originating in the vicinity of the Ancon propagation path and subsequently drifting eastwards to cause the onset of Huancayo scintillation. The other alternative is to consider that the patch had most of its spectral power at kilometer wavelengths and hence could not be detected by the radar. The onset of the second scintillation structure at Ancon was nearly simultaneous with the development of a plume over Jicamarca. In other words, the onset of the second scintillation structure at Ancon cannot be considered to have resulted from an eastward drift of the plume structure over Jicamarca. It seems that Ancon observed two independent irregularity patches which drifted eastwards, causing scintillations at Huancayo, and that the irregularity structure observed at Jicamarca decayed during its transit to Ancon at an ionospheric distance of 350 km to the east of Jicamarca.

It should be mentioned that on this night, scintillation measurements with the 137 - and 360-MHz transmissions from ATS-6 satellite were also conducted at Huancayo. This experiment was conducted because on this night the propagation path from Huancayo to ATS-6 was situated virtually over Jicamarca. Thus the simultaneous radar and scintillation measurements offered an opportunity to examine the relationship between the 3-m and kilometer-sized irregularities over a common ionospheric volume. This has been discussed in Section 3.2.

Figure 8(d) shows the results of ATS-6 scintillation measurements; for ease of comparison, the 50-MHz radar backscatter map is reproduced on the top panel. It may be noted that a single scintillation structure at both frequencies (137 and

360 MHz) was obtained, which agreed very well with the 3-m irregularity structure. It is found that when relatively moderate 3-m irregularities were distributed over a thin layer, weak scintillations were obtained but rather intense 137-MHz scintillation resulted when the irregularity layer was thick, providing a higher value of integrated electron density deviation. It is interesting to note that a single scintillation structure was obtained on the ATS-6 propagation path in contrast to double structures on the propagation paths from Ancon and Huancayo to LES-9. It seems that the first scintillation structure observed at both stations correspond to an irregularity structure that evolved to the east of Jicamarca. As a result, there was no corresponding radar backscatter or ATS-6 scintillations.

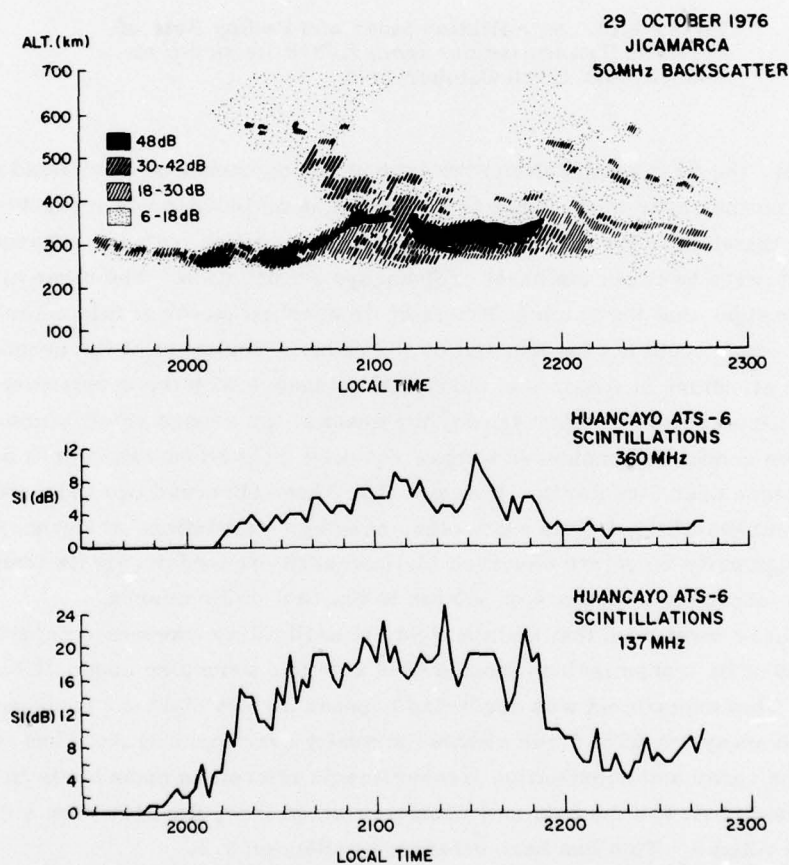


Figure 8(d). Comparison of Backscattered Power Map and ATS-6 Scintillation Data Corresponding to a Common Ionospheric Volume Obtained on 29-30 October 1976

Figure 9 provides a summary diagram of radar and scintillation measurements performed during the October period. Based on the observational statistics, it may be concluded that the number of scintillation structures was much larger than the number of plume structures in the radar. The preponderance of kilometer-sized irregularities causing scintillations, possibly indicates that the turbulent energy does not always cascade down to meter wavelengths.²⁸ Table 2 provides a summary of patch sizes and drift velocities observed from multistation scintillation observations.

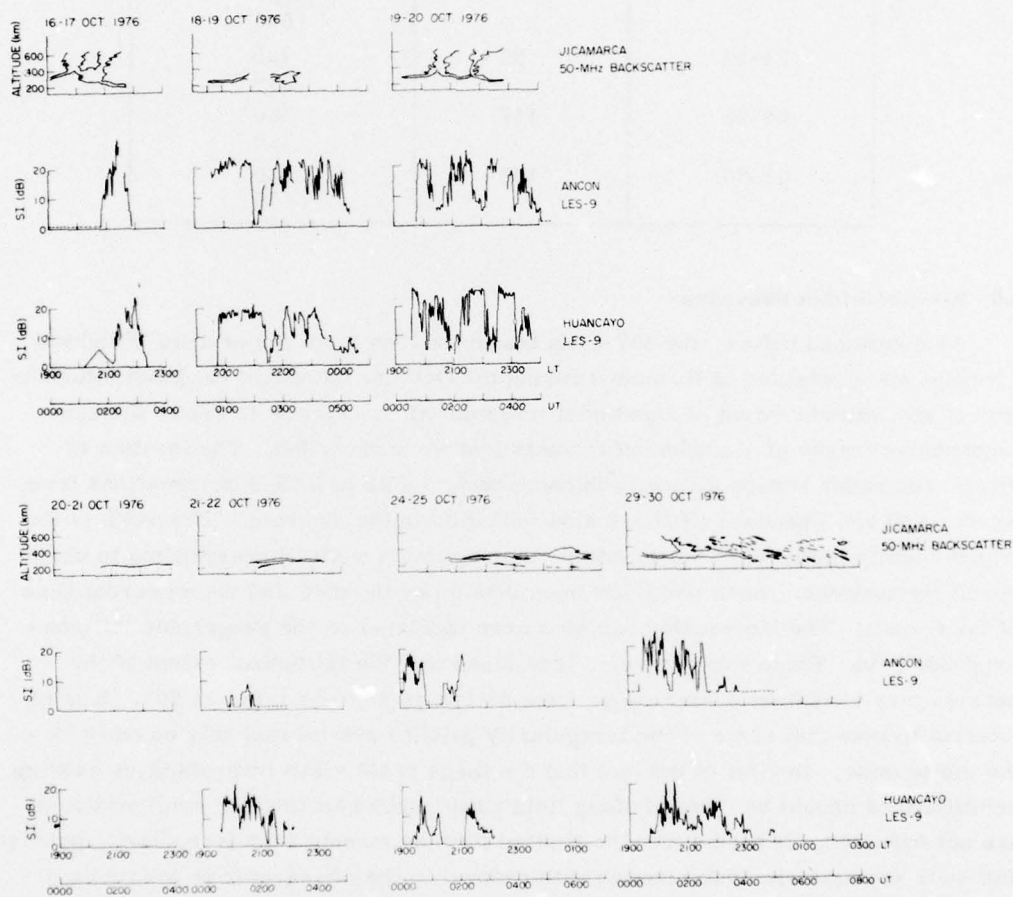


Figure 9. Comparison of Backscattered Power Maps in Schematic Form, and Scintillation Results During the Period of Simultaneous Measurements in October 1976

Table 2. Drift Velocities and East-West Dimensions of Irregularity Patches

Date (October 1976)	Eastward drift speed (m/sec)	Patch dimension (km)
16-17	100 95	360
18-19	116 140	700 1550 (multiple?)
19-20	125	300 330 500 575
21-22	85	180 280
24-25	116	380 410
29-30	100	360 450

4.8 Wideband Satellite Observations

As mentioned before, the 137-MHz transmissions from the orbiting Wideband satellite were received at Huancayo during the October campaign to obtain information on the latitude extent of equatorial irregularities. Figure 10 shows the sub-ionospheric tracks of a number of transits that were recorded. The location of Jicamarca radar station (JI) and subionospheric points of LES-9 observations from Ancon (AN) and Huancayo (HU) are also indicated in the diagram. The width of the tracks signify the level of scintillation, the maximum width corresponding to about 20-dB fluctuations. Each track has been labeled by the date and the universal time of the transit. The dip equator has also been indicated on the geographic latitude-longitude grid. From this diagram, it is found that the latitudinal extent of the patches may vary over a wide range from as low as 4° to as large as 20° . It is of interest to note that some of the irregularity patches are located only on one side of the dip equator. In view of the fact that the large scale sized irregularities causing scintillations should be mapped along field lines, such asymmetric configurations are not expected. It seems that the limited latitude extent of the irregularity patches and their asymmetric configuration with respect to the dip equator is not real but caused by the finite inclination of the Wideband satellite orbit with the magnetic field. Owing to the above orbital constraint and limited E-W dimension of the irregularity patch discussed in Sections 4.1 to 4.7, it is possible for the propagation path to enter the eastern edge of an irregularity patch and emerge from the western

edge during the passage of the satellite over Huancayo. Careful field mapping of irregularities is currently in progress by utilizing simultaneous scintillation, radar, and Wideband satellite data obtained during the equatorial campaign in March 1977.

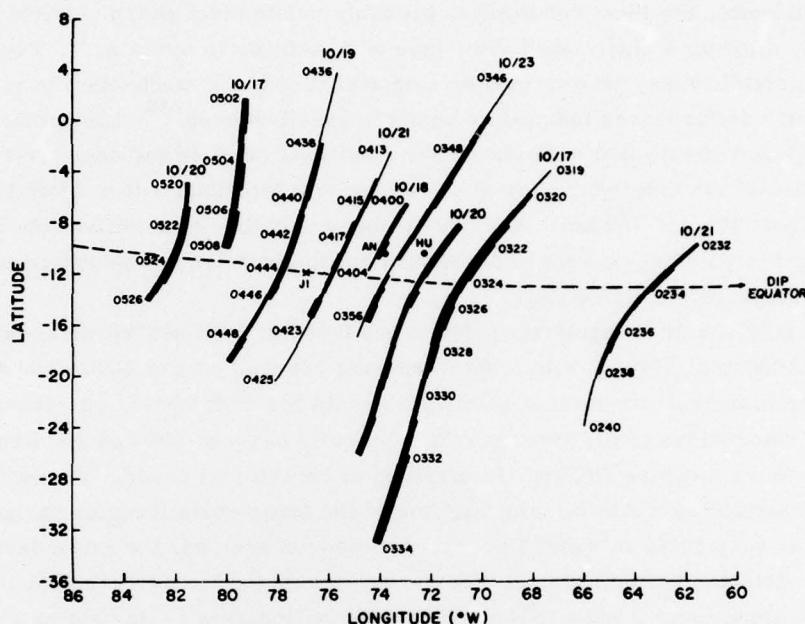


Figure 10. Subionospheric Tracks of Wideband Satellite Transits Recorded at Huancayo During October 1976. Trace thickness indicates the depth of scintillation, maximum thickness corresponding to 20-dB scintillation at 137 MHz. Each track labeled to indicate the date of transit and universal time

5. DISCUSSION

The radar backscatter and scintillation measurements performed near the magnetic equator allowed us to explore a few specific ionospheric locations over an E-W dimension of about 900 km, and thereby obtain information on the large scale features of equatorial irregularity patches.

We find that on certain nights, as on 16-17 October 1976, a single irregularity patch may evolve at a particular location and then drift eastwards for a period dictated by its lifetime. On some other nights, a series of irregularity patches with a large scale quasi-periodicity is observed. A good example of such a configuration was obtained on 19-20 October. Yet, some nights

(20-21 October, 21-22 October) are conspicuous by the absence of any irregularities over the entire 900-km distance explored by the present set of observations. Although the irregularity patches occur after local sunset, these are found to evolve first, either in the west or in the east, signifying that local conditions rather than local time dictate the generation of the irregularities. From a theoretical standpoint, the local condition is probably related to a sharp vertical density gradient, allowing a Rayleigh-Taylor type of instability to operate.¹⁵ The seeding for the instability may be provided by a spatial resonance mechanism in traveling ionospheric disturbances induced by acoustic gravity waves.³⁰ The present set of observations indicate that suitable initial conditions exist either over a very localized region of the ionosphere, or at a few discrete locations with a spatial periodicity of about 300 and 450 km. The day-to-day variability of scintillations is naturally linked to the development of conditions appropriate for the operation of a suitable instability mechanism.

The large scale irregularity patches are found to drift eastwards consistently between 1900 and 2400 LT with a speed ranging between 90 and 140 m per sec. Combining the temporal variation of scintillation with the drift speed, one observes that the E-W dimensions of the patches range typically between 200 and 400 km, although dimensions as large as 700 km are obtained in exceptional cases. These results are summarized in Table 2. The lifetime of the large scale irregularity patches is found to vary between 2 and 3 hours. On many occasions, the irregularity patches, detected by the radar at Jicamarca, occupying the westernmost location, decayed during their transit to the subionospheric location at Marisat at a distance of 900 km. For an average eastward drift speed of 100 m per sec, and an ionospheric distance of 900 km, approximate lifetimes of 3 hours can be attributed to large-scale irregularity patches.

Scintillation measurements with the orbiting Wideband satellite indicated the presence of irregularity patches extending over a latitude interval as large as 20°. Such large latitudinal extents are not surprising as large scale sized irregularities causing scintillations are expected to be highly field aligned. In Figure 10, we have illustrated that, on occasions, irregularity patches are located only on one side of the dip equator; those patches may have extents as small as 4°. It should be mentioned that the Wideband satellite orbit is inclined to the earth's magnetic field even though at a small angle. For such an orbit orientation and for irregularity patches with limited E-W extent, it is possible for the propagation path to enter the eastern edge and emerge from the western edge, giving the impression of patches having asymmetric location and limited N-S extent.

30. Beer, T. (1974) On the dynamics of equatorial spread-F, Australian J. Phys. 27:391-400.

The simultaneous radar and scintillation measurements can, in principle, provide information on the relationship between kilometer-sized irregularities causing scintillations and meter-sized irregularities, giving rise to radar backscatter. It should be mentioned that the two measurements were not conducted over a common ionospheric volume. Yet with the spatial separations involved in the experiment, we were able to show that the irregularity patches which produced radar backscatter drifted eastward, causing scintillations subsequently at several ionospheric locations in the east. This showed that when 3-m irregularities are detected kilometer-sized irregularities are necessarily present, as is expected from theory. A study of Figure 9, indicates that we were able to detect twice as many scintillation structures as the number of plumes in radar maps. The statistical preponderance of kilometer-sized irregularity patches possibly signify that the turbulent energy does not always cascade down to meter scale size.

Based on in situ irregularity and ground scintillation measurements at VHF and S-band, Basu and Basu⁷ showed that the 3-dimensional irregularity power spectrum in the nighttime equatorial F-region follows the power-law variation established by Dyson et al.⁸ The recent results of Woodman and Basu⁴ indicate that the above form of irregularity spectrum probably does not extend to 3-m scale length where the effects of a finite ion-gyro-radius may cause a sharper rolloff of the power spectrum.

The present radar and scintillation studies provided a great deal of information on large scale features of equatorial irregularities such as their localized generation, drift speeds, patch dimensions, and day-to-day variability. It has also raised many fundamental questions regarding the nature of instability mechanisms responsible for the generation of equatorial irregularities and the form of power spectrum. The relationship between large and small sized irregularities could be investigated in a rather qualitative manner, indicating a preponderance of irregularity patches containing only the large scale irregularities.²⁸ A quantitative study of the relationship can be made by making observations over a common ionospheric volume. In the March 1977 campaign, scintillation and radar measurements could be conducted over a common ionospheric volume for an extended period. This later campaign is expected to provide answers to some of the problems discussed here.

References

1. Booker, H. G., and Wells, H. W. (1938) Scattering of radio waves by the F-region of the ionosphere, J. Geophys. Res. 43:249-256.
2. Aarons, J., Whitney, H. E., and Allen, R. S. (1971) Global morphology of ionospheric scintillation, Proc. IEEE 59:159-172.
3. Skinner, N. J., and Kelleher, R. F. (1971) Studies of F-region irregularities at Nairobi, I - From spread-F on ionograms 1964-1970, Ann. Geophys. 27:181-194.
4. Craft, H. D., and Westerlund, L. H. (1972) Scintillation at 4 and 6 GHz caused by the ionosphere, AIAA Paper No. 72-179, American Institute of Aeronautics and Astronautics Library, New York.
5. Hanson, W. B., and Sanatani, S. (1973) Large N_i gradients below the equatorial F-peak, J. Geophys. Res. 78:1167-1173.
6. McClure, J. P., Hanson, W. B., and Hoffman, J. H. (1977) Plasma bubbles and irregularities in the equatorial ionosphere, J. Geophys. Res. 82:2650-2656.
7. Basu, Sunanda, and Basu, Santimay (1976) Correlated measurements of scintillations and in-situ F-region irregularities from OGO-6, Geophys. Res. Lett. 3:681-684.
8. Dyson, P. L., McClure, J. P., and Hanson, W. B. (1974) In-situ measurements of the spectral characteristics of F-region ionospheric irregularities, J. Geophys. Res. 79:1495-1502.
9. Basu, Sunanda, Basu, Santimay, and Khan, B. K. (1976) Model of equatorial scintillations from in-situ measurements, Radio Science 11:821-832.
10. Kelley, M. C., Haerendel, G., Kappler, H., Valenzuela, A., Balsley, B. B., Carter, D. A., Ecklund, W. L., Carlson, C. W., Hausler, B., and Torbert, R. (1976) Evidence for a Rayleigh-Taylor type instability and upwelling of depleted density regions during equatorial spread-F, Geophys. Res. Lett. 3:448-450.
11. Morse, F. A., Edgar, B. C., Koons, H. C., Rice, C. J., Heikkila, W. J., Hoffman, J. H., Tinsley, B. A., Winningham, J. D., Christiansen, A. B., Woodman, R. F., Pomalaza, J., and Teixeira, N. R. (1977) Equion: an equatorial ionospheric irregularity experiment, J. Geophys. Res. 82:578-592.

References

12. Woodman, R.F., and La Hoz, C. (1976) Radar observations of F-region equatorial irregularities, J. Geophys. Res. 81:5447-5466.
13. Röttger, J. (1976) The macroscale structure of equatorial irregularities, J. Atmos. Terr. Phys. 38:97-101.
14. Scannapieco, A.J., and Ossakow, S.L. (1976) Nonlinear equatorial spread-F, Geophys. Res. Lett. 3:451-454.
15. Haerendel, G. (1974) Theory of equatorial spread-F, Preprint, Max-Planck-Institut für Physik und Astrophysik, Garching, West Germany.
16. Hudson, M.K., and Kennel, C.F. (1975) Linear theory of equatorial spread-F, J. Geophys. Res. 80:4581-4590.
17. Basu, Sunanda, and Kelley, M.C. (1977) Review of equatorial scintillation phenomena in the light of recent developments in the theory and measurement of equatorial irregularities, J. Atmos. Terr. Phys. 39:1229-1242.
18. Whitney, H.E., Aarons, J., and Malik, C. (1969) A proposed index for measuring ionospheric scintillations, Planet. Space Sci. 17:1069-1073.
19. Briggs, B.H., and Parkin, I.A. (1963) On the variation of radio star and satellite scintillation with zenith angle, J. Atmos. Terr. Phys. 25:339-366.
20. Rufenach, C.L. (1975) Ionospheric scintillation by a random phase screen; spectral approach, Radio Sci. 10:155-165.
21. Costa, E., and Kelley, M.C. (1976) Calculations of equatorial scintillations at VHF and GHz frequencies based on a new model of the disturbed equatorial ionosphere, Geophys. Res. Lett. 3:677-680.
22. Yeh, K.C., Liu, C.H., and Youakim, M.Y. (1975) A theoretical study of the ionospheric scintillation behavior caused by multiple scattering, Radio Sci. 10:97-106.
23. Booker, H.G. (1956) A theory of scattering by nonisotropic irregularities with application to radar reflections from the aurora, J. Atmos. Terr. Phys. 8:204-221.
24. Woodman, R.F., and Basu, Sunanda (1977) Comparison between in-situ spectral measurements of equatorial F-region irregularities and backscatter observations at 3 m wavelength (abstract), EOS Trans. AGU, 58:449.
25. Woodman, R.F. (1972) East-west ionospheric drifts at the magnetic equator, Space Research XII, Akademie-Verlag, Berlin, pp 968-974.
26. Prokhorov, A.M., Bunkin, F.V., Gochilashvily, K.S., and Shishov, V.I. (1975) Laser irradiance propagation in turbulent media, Proc. IEEE 63:790-811.
27. Aarons, J., Buchau, J., Basu, Santimay, and McClure, J.P. (1978) The localized origin of equatorial F-region irregularity patches, J. Geophys. Res. (to be published).
28. Basu, Santimay, Aarons, J., McClure, J.P., and Calderon, C. (1977) Combined study of nighttime equatorial irregularities by radar backscatter, ground-based and airborne scintillation measurements (abstract), EOS Trans. AGU 58:450.
29. Balsley, B.B., and Farley, D.T. (1975) Partial reflections: A source of weak VHF equatorial spread-F echoes, J. Geophys. Res. 80:4735-4737.
30. Beer, T. (1974) On the dynamics of equatorial spread-F, Australian J. Phys. 27:391-400.